Supplementary Information for

Synthesis of Macrocyclic Salen Rare-Earth Complexes and Their Framework Conversion Regulated by Coordination Sphere Engineering

Yi-Fu Liu[a], Guzmán Gil-Ramírez*[b], Takashi Nakamura*[c]

[a]Degree Programs in Pure and Applied Sciences, Graduate School of Science and Technology, University of Tsukuba, 1-1-1 Tennodai, Tsukuba, Ibaraki 305-8571, Japan.

[b]School of Chemistry, University of Lincoln, Joseph Banks Laboratories, Lincoln LN6 7DL, United Kingdom.

[c]Institute of Pure and Applied Sciences, University of Tsukuba, 1-1-1 Tennodai, Tsukuba, Ibaraki 305-8571, Japan.

*Corresponding Authors. E-mail: GGilramirez@lincoln.ac.uk (Guzmán Gil-Ramírez)

nakamura@chem.tsukuba.ac.jp (Takashi Nakamura)

Table of Contents

Materials and Methods

Unless otherwise noted, solvents and reagents were purchased from Tokyo Chemical Industry Co., Ltd., Fujifilm Wako Pure Chemical Co., Kanto Chemical Co., Inc., Nacalai Tesque, Inc. or Sigma-Aldrich Japan G.K., and used without further purification. Dry THF and DMF were purified by Glass Contour Ultimate Solvent System. Silica gel for column chromatography was purchased from Kanto Chemical Co. Inc. (Silica Gel 60 N (spherical, 63–210 μm)). Automated flash chromatography purifications were performed using a Biotage Isolera One system with Biotage Sfär Silica (HC D 20 mm) columns.

Measurements were performed at 298 K unless otherwise noted. ^{1}H NMR spectra were recorded on Bruker AVANCE III-600 spectrometers. ESI TOF mass data were recorded on an AB SCIEX TripleTOF 4600 system. UV-Vis spectra were recorded on a JASCO V-670 spectrophotometer. Emission spectra were recorded on a JASCO FP-8600 fluorescence spectrophotometer. Absolute fluorescence quantum yields were determined with a Hamamatsu Photonics absolute PL quantum yield measurement system C9920-02.

Single-crystal X-ray crystallographic measurements were performed using Bruker APEX II ULTRA with Mo Kα radiation at 100 K. Obtained data were collected using Bruker APEX2[S1a] and processed using Bruker APEX3[S1b] and Yadokari-XG[S2] crystallographic software package. The initial structures were solved using SHELXT-2018[S3], and refined using SHELXL-2018[S4].

We appreciate the Organization for Open Facility Initiatives (Univ. of Tsukuba) for the NMR and ESI TOF mass measurements.

Synthesis of Complexes

Scheme S1. Preparation of **1a**Y_3X_n

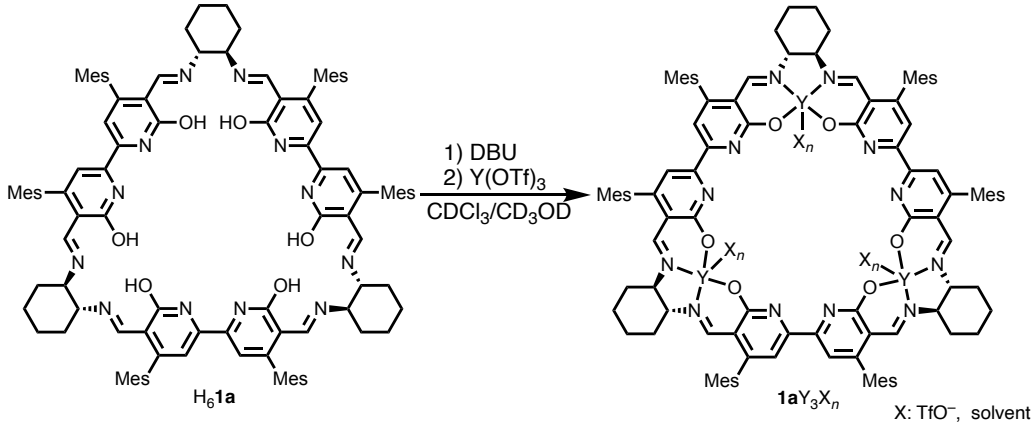

Preparation of **1a**Y_3X_n

H_6**1a**[S5] (15.0 mg, 8.9 μmol), $CDCl_3$ (412.5 μL), and CD_3OD (137.5 μL) were added to an NMR tube, which resulted in a clear yellow solution. Next, 1,8-diazabicyclo[5,4,0]undec-7-ene (DBU) (10.6 mg, 69.8 μmol), $CDCl_3$ (99 μL), and CD_3OD (33 μL) were added to a microtube. The solution of DBU (100 μL, 53.0 μmol) was added to the NMR tube. The color of the solution changed from yellow to orange as the NMR tube was shaken by hand at room temperature for 1 min. To another microtube, $Y(OTf)_3$ (41.1 mg, 74.8 μmol), $CDCl_3$ (187 μL), and CD_3OD (63 μL) were added. The solution of $Y(OTf)_3$ (190 μL, 55.1 μmol) were added to the NMR tube, which resulted in the orange solution of the Y complex. The formation of **1a**Y_3X_n (X: TfO^- or solvent) was confirmed by ^1H NMR (**Figure S1**) and ESI TOF mass (**Figure S2**) measurements.

^1H NMR (600 MHz, $CDCl_3/CD_3OD$ = 3/1): δ 7.95 (s, 6H), 7.06 (s, 6H), 6.96 (s, 6H), 6.94 (s, 6H), 2.33 (s, 18H), 2.02 (s, 18H), 1.97 (s, 18H). The signals of cyclohexane unit were overlapped with DBU.

HRMS (ESI): observed *m*/*z* 795.4828 ([**1a**$Y_3(HOTf)_3$]$^{3+}$). Calcd. 795.4839.

Scheme S2. Formation of **1b**Y_4X_n

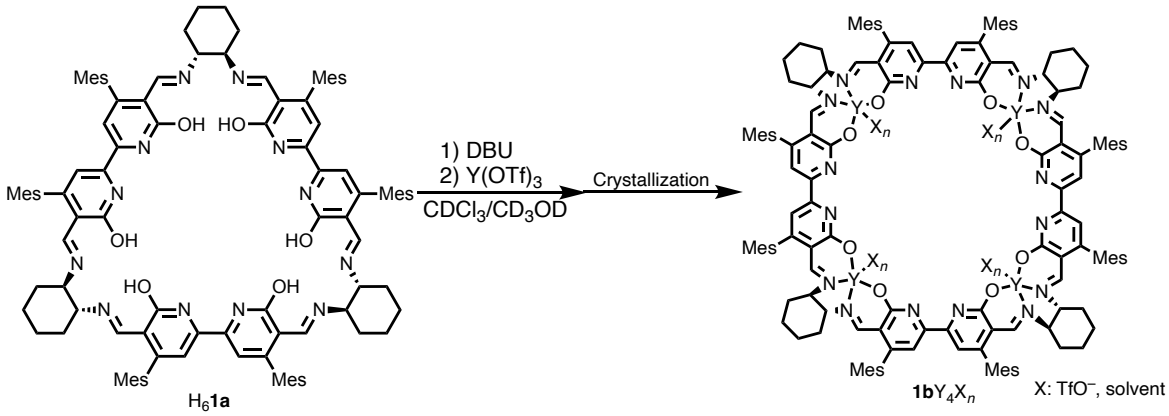

Formation of **1b**Y_4X_n

H_6**1a** (16.5 mg, 9.8 μmol), $CDCl_3$ (412.5 μL), and CD_3OD (137.5 μL) were added to an NMR tube, which resulted in a clear yellow solution. Next, 1,8-diazabicyclo[5,4,0]undec-7-ene (DBU) (20.6 mg, 135.2 μmol), $CDCl_3$ (207 μL), and CD_3OD (69 μL) were added to a microtube. The solution of DBU (120 μL, 58.9 μmol) was added to the NMR tube. The color of the solution changed from yellow to orange as the NMR tube was shaken by hand at room temperature for 1 min. To another microtube, $Y(OTf)_3$ (31.94 mg, 70.8 μmol), $CDCl_3$ (190 μL), and CD_3OD (63 μL) were added. The solution of $Y(OTf)_3$ (210 μL, 58.9 μmol) was added to the NMR tube, which resulted in the orange solution of the Y complex. The formation of trimer **1a**Y_3X_n was confirmed by ^{1}H NMR. Tetramer **1b**Y_4X_n (X: TfO^- or solvent) with DBU salt (total 13.95 mg) was obtained by slow vapor diffusion of diisopropyl ether into the solution of trimer **1a**Y_3X_n dissolved in $CHCl_3/CH_3OH$ = 3/1 (3 mL) The formation of **1b**Y_4X_n was confirmed by ^{1}H NMR (**Figure S3**), ESI mass (**Figure S5**), and single-crystal X-ray diffraction (**Figure S8**) measurements.

^{1}H NMR (600 MHz, $CDCl_3/CD_3OD$ = 3/1): δ 8.08 (s, 8H), 7.08 (s, 8H), 6.98 (s, 8H), 6.97 (s, 8H), 2.34 (s, 24H), 2.04 (s, 24H), 2.01 (s, 24H). The signals of cyclohexane unit were overlapped with DBU.

HRMS (ESI): observed *m*/*z* 606.5292 ([**1b**Y_4 + 3HOTf + H]$^{5+}$). Calcd. 606.5298.
observed *m*/*z* 795.4006 ([**1b**Y_4 + 4HOTf]$^{4+}$). Calcd. 795.4003.
observed *m*/*z* 1110.1848 ([**1b**Y_4 + 4HOTf + OTf]$^{3+}$). Calcd. 1110.1844.

Scheme S3. Preparation of **1a**Lu_3X_n

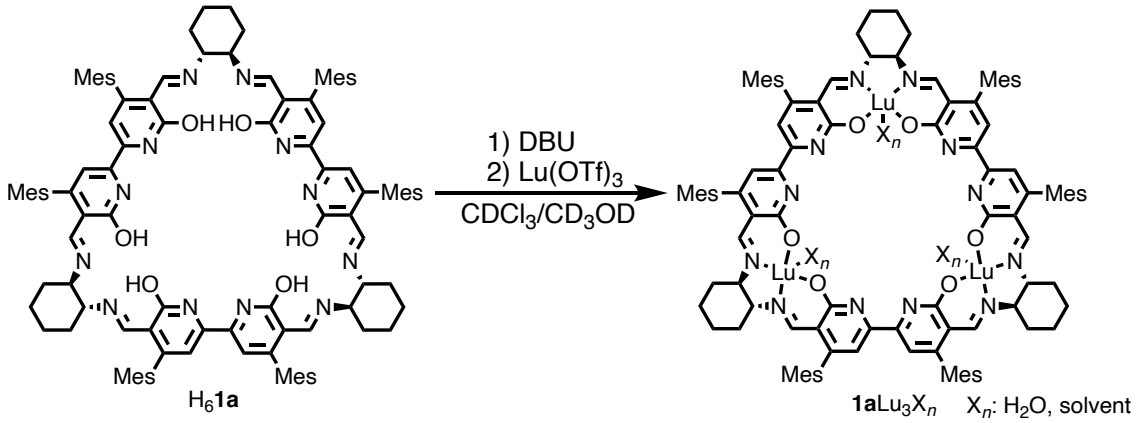

Preparation of **1a**Lu_3X_n

H_6**1a** (11.7 mg, 7.0 μmol), $CDCl_3$ (412.5 μL), and CD_3OD (137.5 μL) were added to an NMR tube, which resulted in a clear yellow solution. Next, 1,8-diazabicyclo[5,4,0]undec-7-ene (DBU) (15.7 mg, 103 μmol), $CDCl_3$ (110.0 μL), and CD_3OD (37.0 μL) were added to a microtube. The solution of DBU (60.0 μL, 42.0 μmol) was added to the NMR tube. The color of the solution changed from yellow to orange as the NMR tube was shaken by hand at room temperature for 1 min. To another microtube, $Lu(OTf)_3$ (26.6 mg, 42.7 μmol), $CDCl_3$ (139.5 μL), and CD_3OD (46.5 μL) were added. The solution of $Lu(OTf)_3$ (183 μL, 42 μmol) were added to the NMR tube, which resulted in the orange solution of the Lu complex. The formation of **1a**Lu_3X_n (X: H_2O or solvent) was confirmed by ^1H NMR (**Figure S10**) and ESI TOF mass (**Figure S11**) measurements.

^1H NMR (600 MHz, $CDCl_3/CD_3OD$ = 3/1): δ 7.95 (s, 6H), 7.06 (s, 6H), 6.96 (s, 6H), 6.94 (s, 6H), 2.33 (s, 18H), 2.02 (s, 18H), 1.97 (s, 18H). The signals of cyclohexane unit were overlapped with DBU.

HRMS (ESI): observed *m*/*z* 698.8813 ([**1a**Lu_3 + 4HOTf + H]$^{4+}$). Calcd. 698.8810.

Scheme S4. Formation of **1b**Lu_4X_n

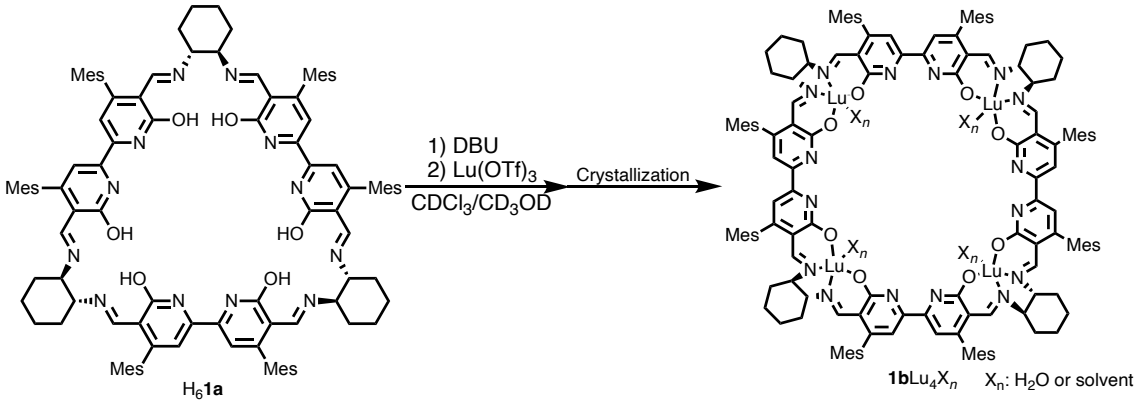

Formation of **1b**Lu_4X_n

H_6**1a** (17.9 mg, 10.7 μmol), $CDCl_3$ (412.5 μL), and CD_3OD (137.5 μL) were added to an NMR tube, which resulted in a clear yellow solution. Next, 1,8-diazabicyclo[5,4,0]undec-7-ene (DBU) (15.6 mg, 103 μmol), $CDCl_3$ (18 μL), and CD_3OD (6 μL) were added to a microtube. The solution of DBU (15 μL, 64 μmol) was added to the NMR tube. The color of the solution changed from yellow to orange as the NMR tube was shaken by hand at room temperature for 1 min. To another microtube, $Lu(OTf)_3$ (42.5 mg, 68.3 μmol), $CDCl_3$ (189 μL), and CD_3OD (63 μL) were added. The solution of $Lu(OTf)_3$ (240 μL, 64.2 μmol) was added to the NMR tube, which resulted in the orange solution of the Lu complex. The formation of trimer **1a**Lu_3X_n was confirmed by ^{1}H NMR. Tetramer **1b**Lu_4X_n (X: H_2O or solvent) with DBU salt (total 9.8 mg) was obtained by slow vapor diffusion of diisopropyl ether into the solution of trimer **1a**Lu_3X_n dissolved in $CHCl_3/CH_3OH$ = 3/1 (5 mL). The formation of **1b**Lu_4X_n was confirmed by ^{1}H NMR (**Figure S14**) and single-crystal X-ray diffraction (**Figure S16**) measurements.

^{1}H NMR (600 MHz, $CDCl_3/CD_3OD$ = 3/1): δ 7.97 (s, 8H), 7.11 (s, 8H), 6.98–6.95 (16H), 2.33 (s, 24H), 2.02 (s, 24H), 1.98 (s, 24H). The signals of cyclohexane unit were overlapped with DBU.

As in the case of Y, after leaving the solution of the trimer [**1a**Lu_3X_n] prepared by mixing H_6**1a** and $LuOTf)_3$ at room temperature or at 50°C for 72 h, it was observed by ^{1}H NMR measurements that the trimer remained as the main component. However, broad signals that were not assigned to neither trimer nor tetramer appeared when heated at 50°C for 72 h. The transition from trimer to tetramer occurs only during the crystallization process. (**Figure S12, S13**).

Scheme S5. Synthesis of [**1a**Lu_3**2**$_3$]

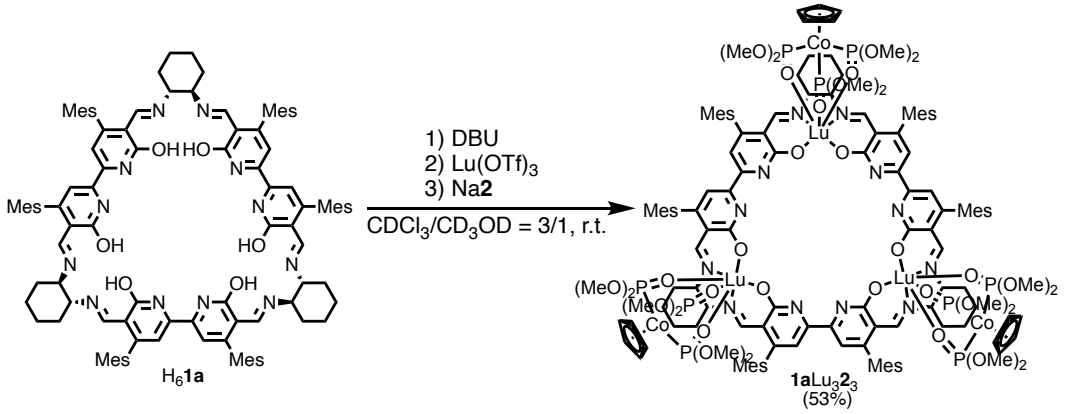

Synthesis of [**1a**Lu_3**2**$_3$]

H_6**1a** (17.9 mg, 10.7 μmol), $CDCl_3$ (412.5 μL), and CD_3OD (137.5 μL) were added to an NMR tube, which resulted in a clear yellow solution. DBU (21.1 mg, 138.8 μmol), $CDCl_3$ (16.5 μL), and CD_3OD (5.5 μL) were added to a microtube, and the solution of DBU (10.0 μL, 64.0 μmol) was added to the NMR tube. The color of the solution changed from yellow to orange as the NMR tube was shaken by hand at room temperature for 1 min. To another microtube, $Lu(OTf)_3$ (42.9 mg, 68.9 μmol), $CDCl_3$ (193.5 μL) and CD_3OD (64.5 μL) were added. The solution of $Lu(OTf)_3$ (240 μL, 64.0 μmol) was added to the NMR tube. Next, Na**2**[S6] (32.7 mg, 69.1 μmol), $CDCl_3$ (194.5 μL) and CD_3OD (64.5 μL) were added to another microtube. The solution of Na**2** (240 μL, 64.01 μmol) was added to the NMR tube. The solvent was evaporated to give a yellow solid (119.6 mg). The yellow solid was dissolved in $CHCl_3$, and the solution was passed through a membrane filter. The yellow solid (87.5 mg) obtained after the evaporation of the solvents was purified by automated column chromatography ($CHCl_3/CH_3OH$ = 1/0–1/1) to give 20.40 mg of yellow solid, which was mainly [**1a**Lu_3**2**$_3$]. The solid was dissolved in $CHCl_3/CH_3OH$ = 3/1 (3 mL) and the vapor of cyclohexane was diffused into the solution over 3 days. The obtained crystals were separated by decantation, washed with cyclohexane, and dried in vacuo to give [**1a**Lu_3**2**$_3$] (18.60 mg, 5.71 μmol, 53%).

See **Figure S19** for the ^{1}H NMR spectrum.

^{1}H NMR (600 MHz, $CDCl_3/CD_3OD$ = 3/1): δ 8.01–7.82 (6H), 7.18–7.14 (6H), 7.01–6.97 (12H), 5.23–5.16 (15H), 3.68–3.63 (54H), 2.35–2.33 (18H), 2.02–1.94 (18H). The signals of cyclohexane unit were overlapped with DBU.

UV ($CHCl_3$): λ_{max} 414 nm ($\varepsilon = 9 \times 10^4$ [$M^{-1}\cdot cm^{-1}$]);

FL ($CHCl_3$): λ_{max} 498 nm (λ_{ex} = 414 nm);

Emission quantum yield ($CHCl_3$): Φ_F = 0.054 (λ_{ex} = 414 nm);

HRMS (ESI): observed *m*/*z* 887.9193 ([**1a**Lu_3**2**$_3$] + 4H)$^{4+}$. Calcd. 887.9186.

Scheme S6. Conversion from tetramer **1b**Lu_4X_n to trimer [**1a**Lu_3**2**$_3$]

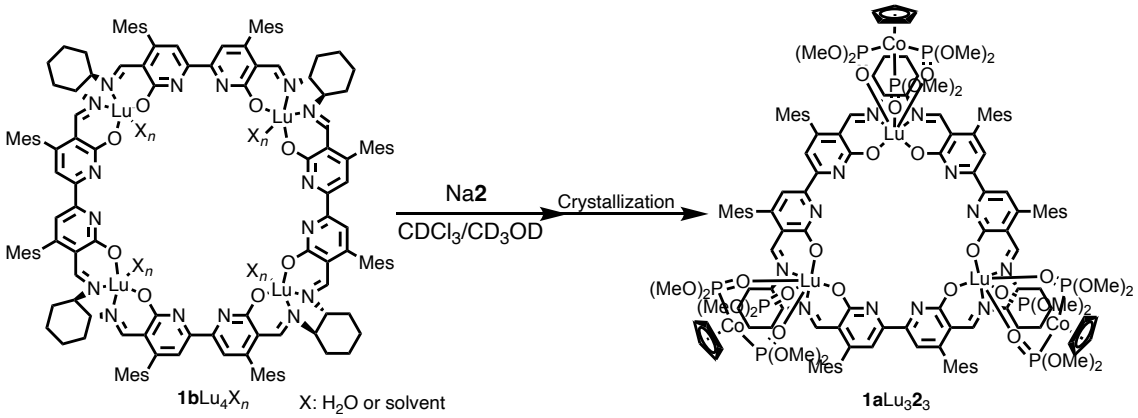

1bLu_4X_n (2.96 mg) synthesized as described in **Scheme S4**, $CDCl_3$ (412.5 μL), and CD_3OD (137.5 μL) were added to an NMR tube, which resulted in a clear yellow solution. Na**2** (2.83 mg, 6.07 μmol), $CDCl_3$ (45 μL) and CD_3OD (15 μL) were added to a microtube. The solution of Na**2** (40 μL, 4.04 μmol) was added to the NMR tube. Next, the solution was passed through a membrane filter. The vapor of cyclohexane was diffused into the solution over 3 days. The obtained crystals were separated by decantation, washed with cyclohexane, and dried in vacuo to give [**1a**Lu_3**2**$_3$], which was characterized by X-ray diffraction analysis.

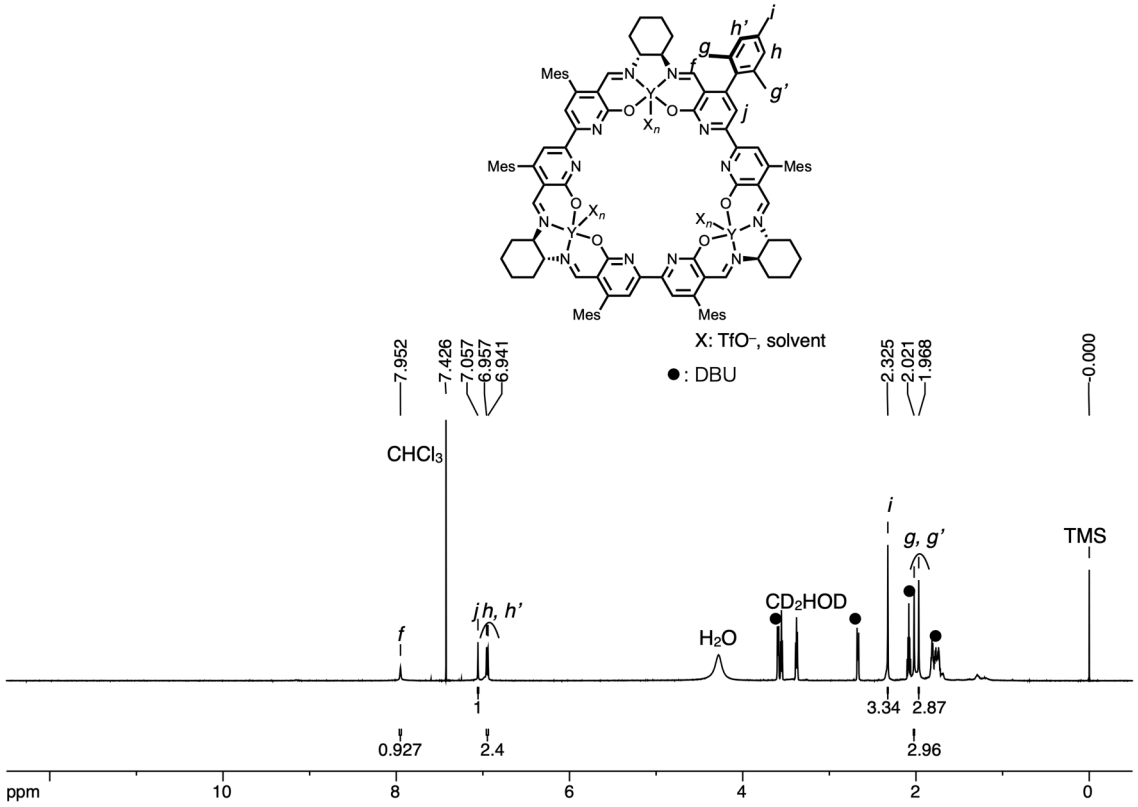

Figure S1. ^{1}H NMR spectrum of **1a**Y_3X_n (X: TfO^- or solvent) ($CDCl_3/CD_3OD$ = 3/1, 600 MHz).

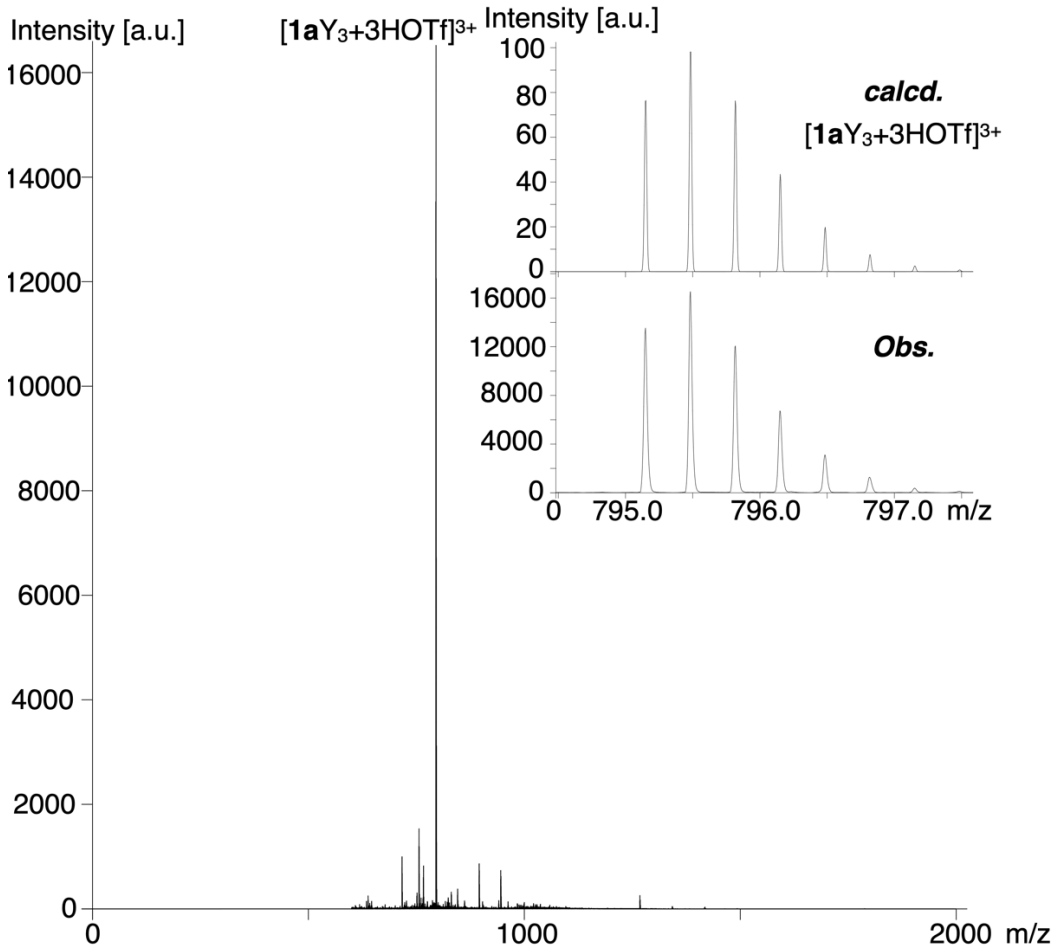

Figure S2. ESI TOF mass spectrum of **1a**Y_3X_n (positive, CH_3CN, 5 μM).

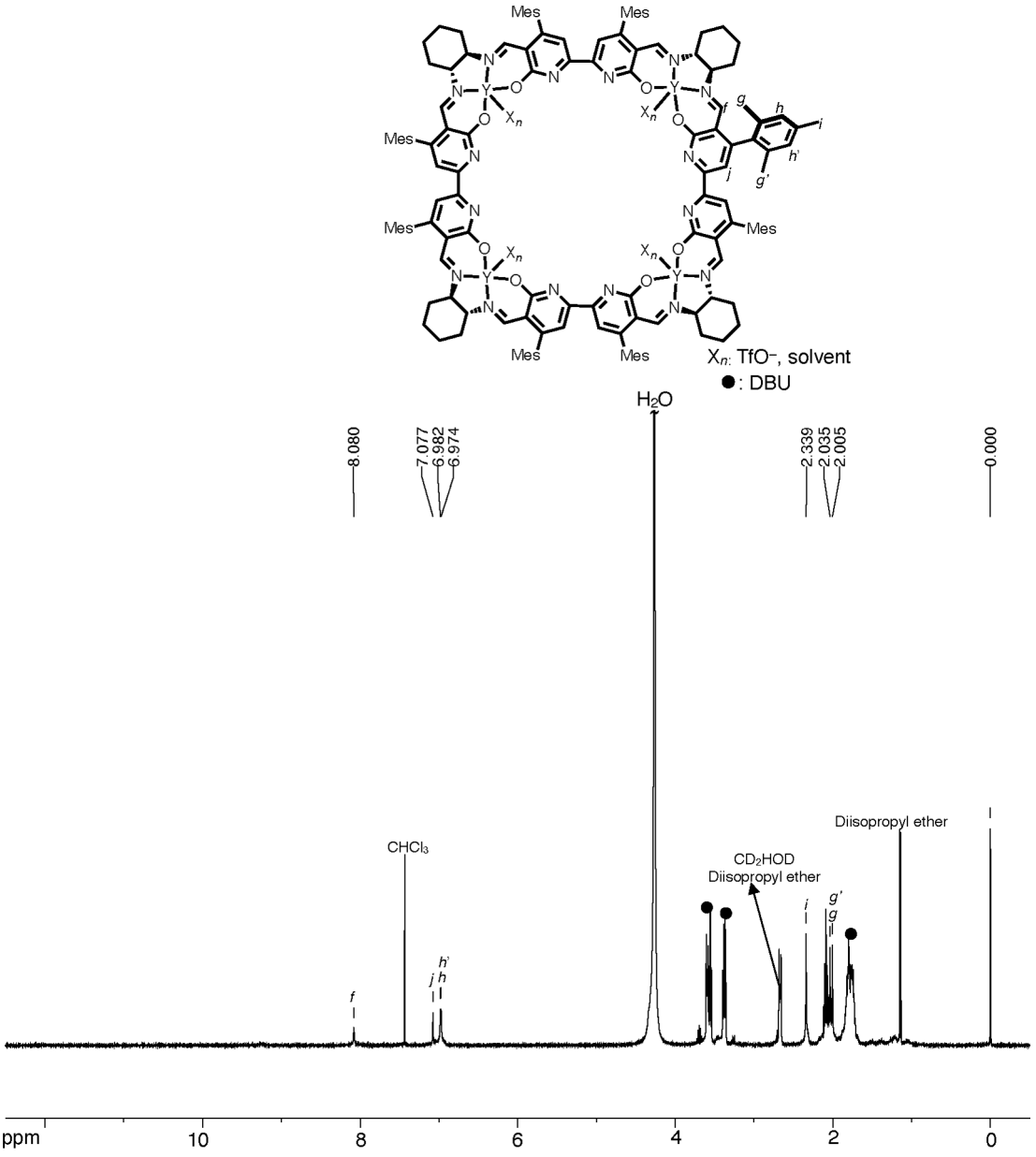

Figure S3. ^{1}H NMR spectrum of **1b**Y_4X_n (X: TfO^- or solvent) ($CDCl_3/CD_3OD$ = 3/1, 600 MHz).

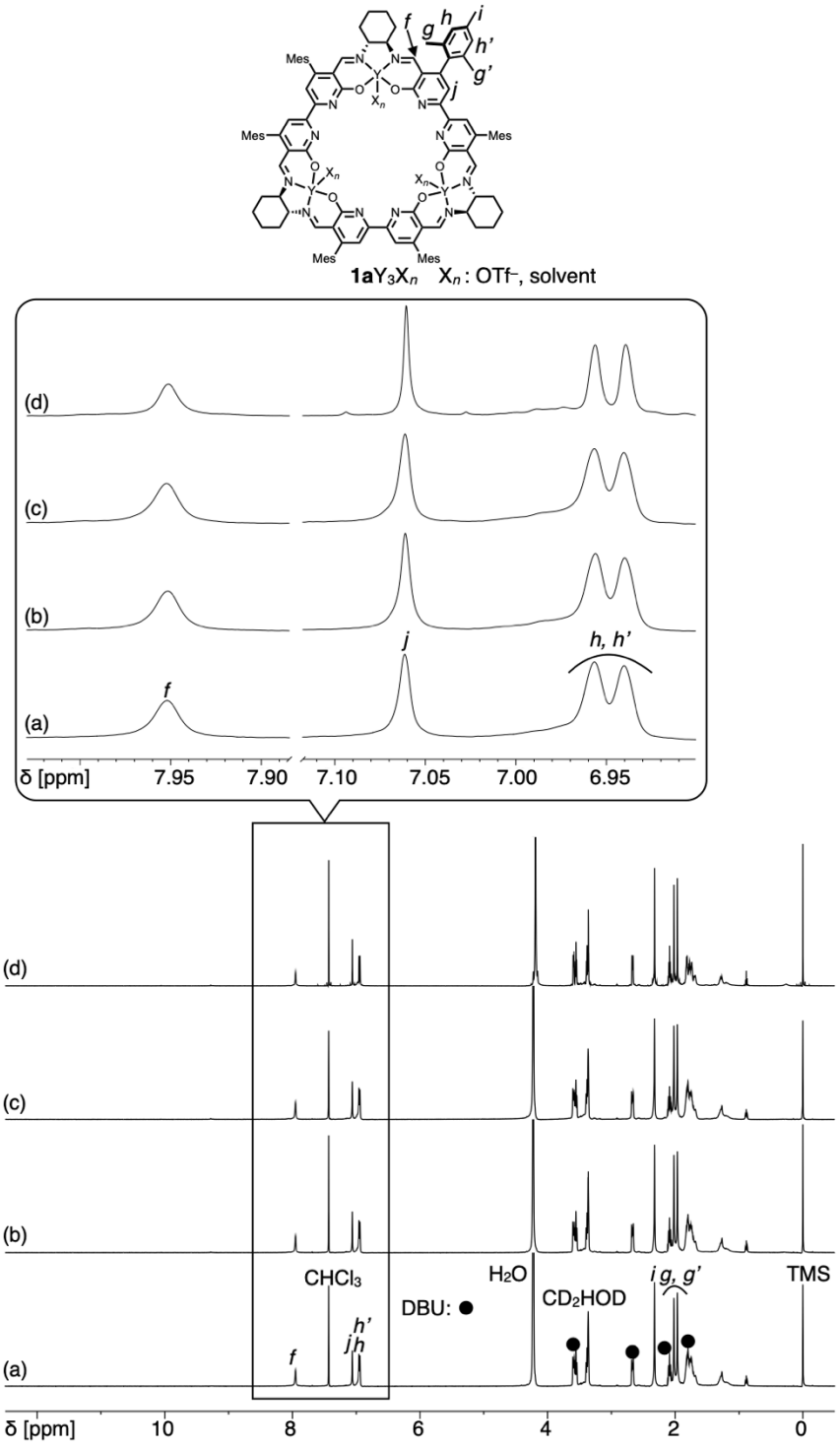

Figure S4. Stability of trinuclear Y complex at room temperature (^{1}H NMR, $CDCl_3/CD_3OD$ = 3/1, 400 MHz). (a) Trimer **1a**Y_3X_n prepared from H_6**1a,** $Y(OTf)_3$, and DBU. (b–d) The sample of (a) stood at r.t. (b) 14 h. (c) 46 h. (d) 72 h.

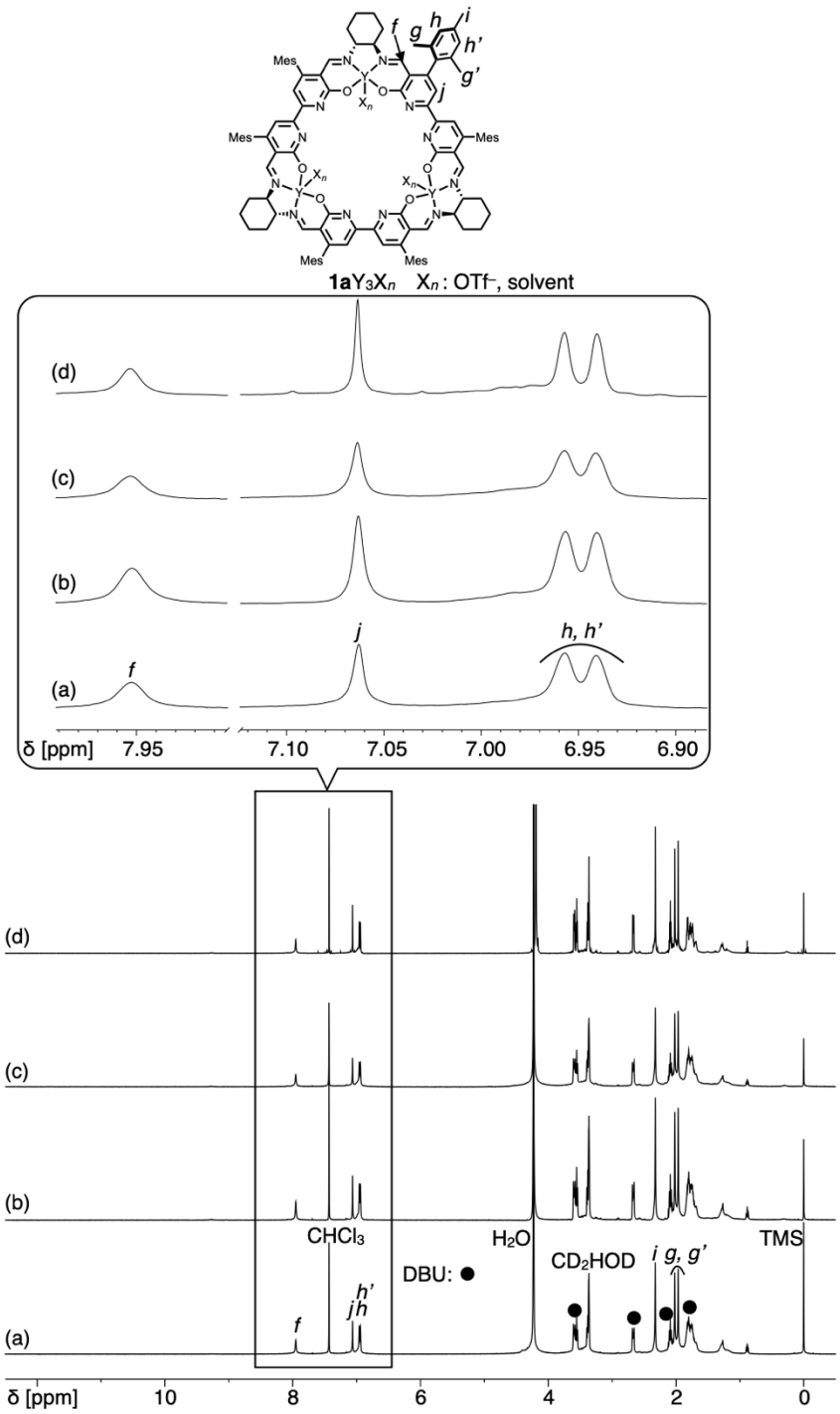

Figure S5. Stability of trinuclear Y complex at 50 °C (^{1}H NMR, $CDCl_3/CD_3OD$ = 3/1, 400 MHz) (a) Trimer **1a**Y_3X_n prepared from H_6**1a,** $Y(OTf)_3$, and DBU. (b–d) The sample of (a) heated at 50 °C (b) 14 h. (c) 46 h. (d) 72 h.

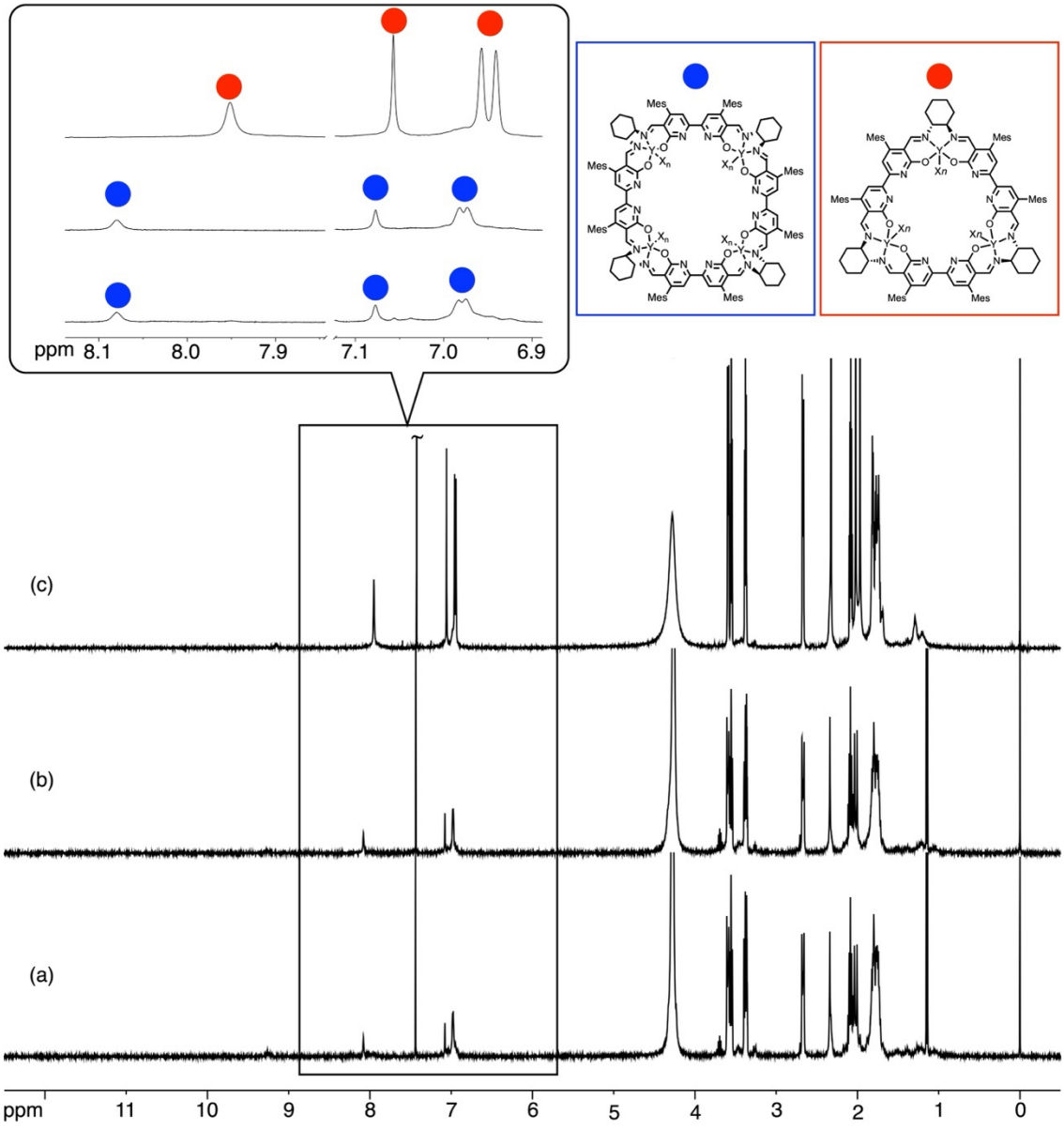

Figure S6. Conversion and stability of macrocyclic complexes (^{1}H NMR, $CDCl_3/CD_3OD$ = 3/1, 600 MHz). (a) Tetramer **1b**Y_4X_n prepared by the dissolution of the crystal. (b) The sample of (a) heated at 50 °C for 1 h. Tetramer **1b**Y_4X_n was retained. (c) Trimer **1a**Y_3X_n prepared from H_6**1a** and $Y(OTf)_3$.

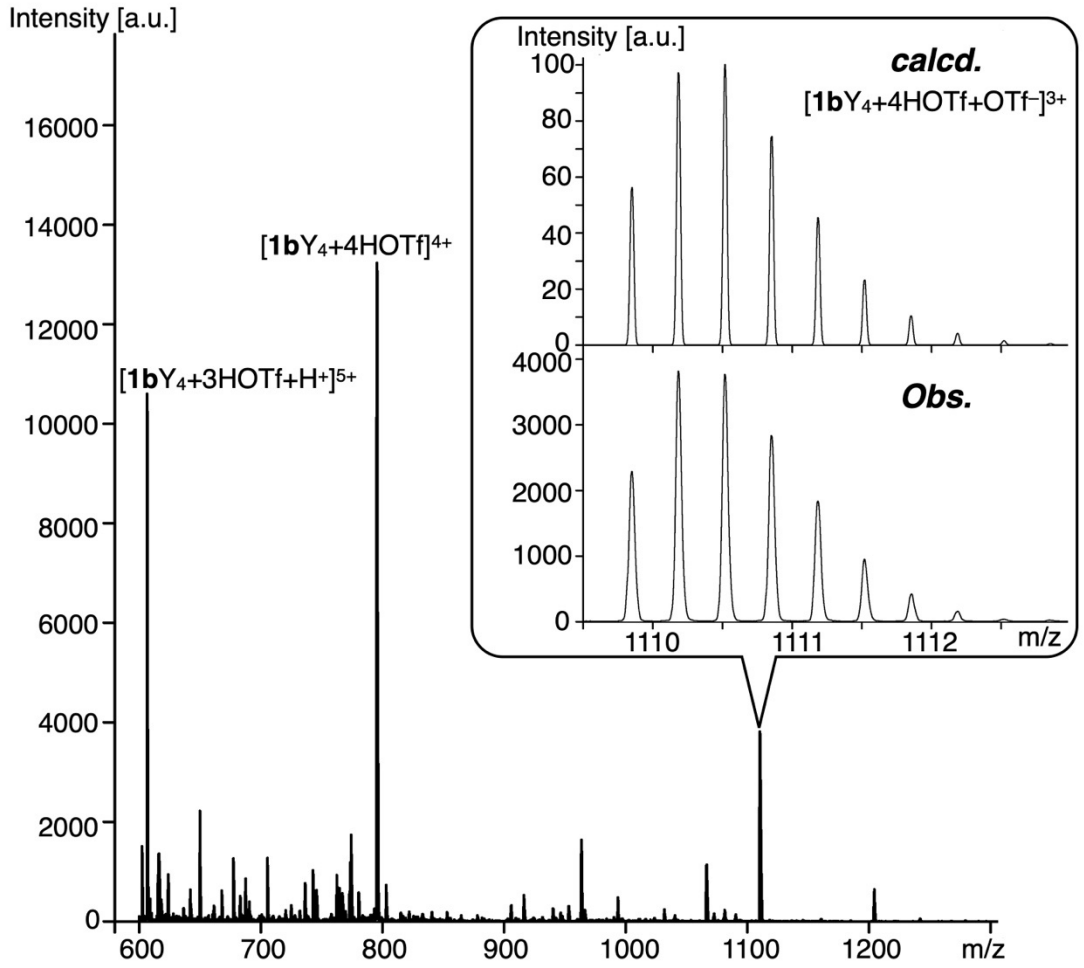

Figure S7. ESI TOF mass spectrum of **1b**Y_4X_n (positive, CH_3CN, 5 μM).

Single crystals of [**1b**$Y_4(H_2O)_{14}(OTf)_2$]$(OTf)_2$ suitable for X-ray diffraction analysis were obtained by slow diffusion of diisopropyl ether vapors into a mixture of H_6**1a**, DBU, and $Y(OTf)_3$ in $CHCl_3/CH_3OH$ = 3/1.

Crystallographic data for [**1b**$Y_4(H_2O)_{14}(OTf)_2$]$(OTf)_2$: $C_{148}H_{172}F_{12}N_{16}O_{34}S_4Y_4$, Fw = 3430.89, yellow prism, 0.60 × 0.15 × 0.06 mm^3, orthorhombic, space group $P2_12_12$ (No. 18), a = 10.1914(19) Å, b = 31.770(6) Å, c = 32.931(6) Å, V = 10662(3) Å^3, θ_{max} = 23.250°, Z = 2, R_1 = 0.1053 ($I > 2\sigma$, after SQUEEZE), wR_2 = 0.2968 (all, after SQUEEZE), Flack parameter 0.054(5), GOF = 1.049. CCDC 2374258.

Solvent accessible voids of 3184 cubic angstroms (29.9% of the unit cell volume) were found, where solvent molecules were heavily disordered. The residual electron density was treated with SQUEEZE[S7]. DFIX, DANG, RIGU, and ISOR restraints were applied for the atoms of TfO^- anions. DANG and RIGU restraints were applied for one mesityl group. The benzene ring of the mesityl group was fixed with AFIX 66.

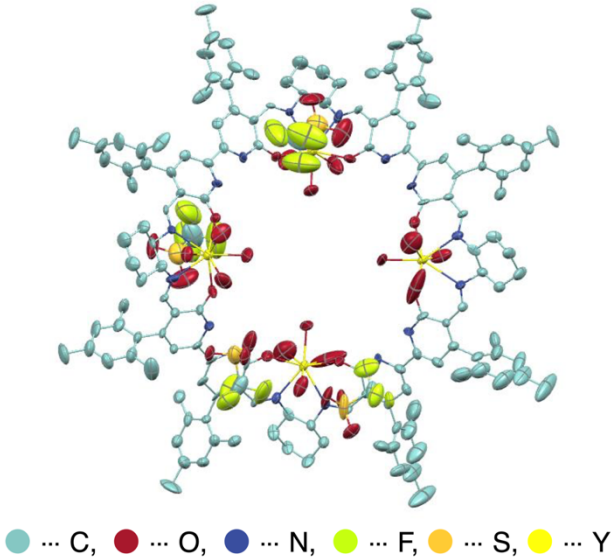

Figure S8. The molecular structure of [**1b**$Y_4(H_2O)_{14}(OTf)_2$]$(OTf)_2$ determined by X-ray diffraction analysis. An ellipsoidal model (50% probability). Hydrogen atoms were omitted for clarity.

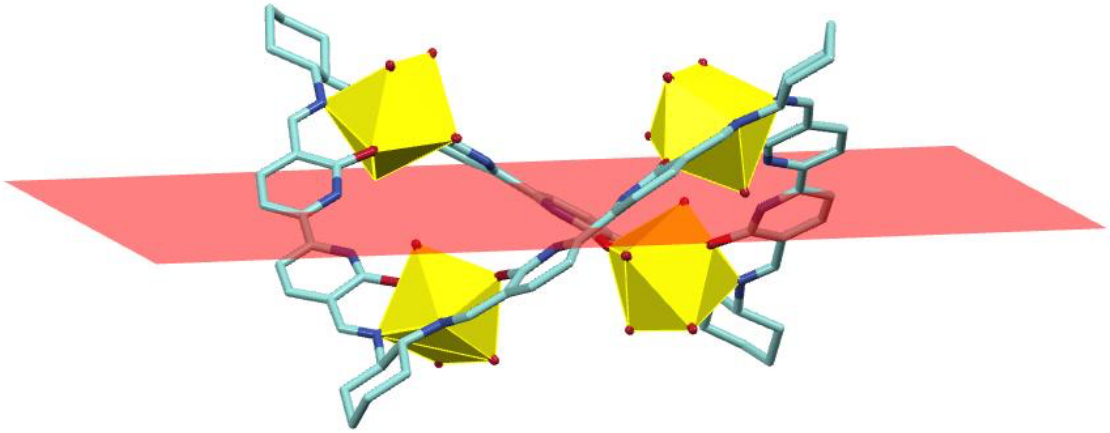

Figure S9. Least-squares plane (red) defined by four Y atoms of [**1b**$Y_4(H_2O)_{14}(OTf)_2$]$(OTf)_2$.

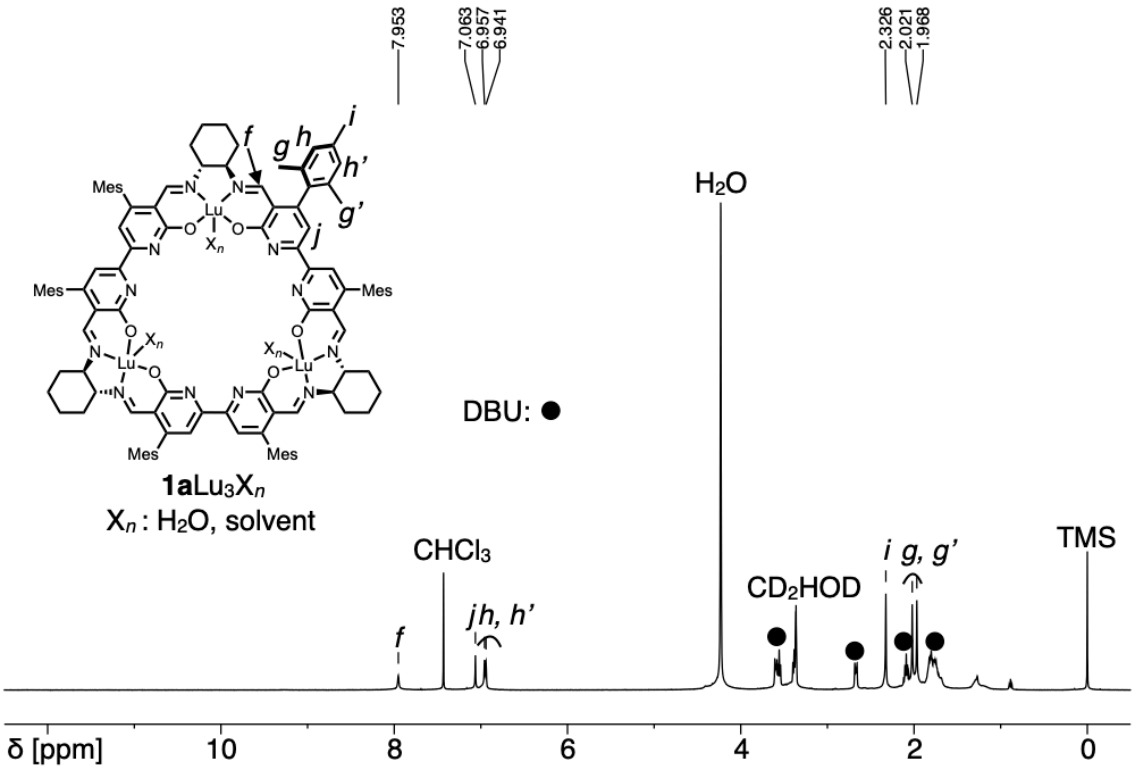

Figure S10. ^{1}H NMR spectrum of **1a**Lu_3X_n (X: H_2O or solvent) ($CDCl_3$/CD_3OD = 3/1, 600 MHz).

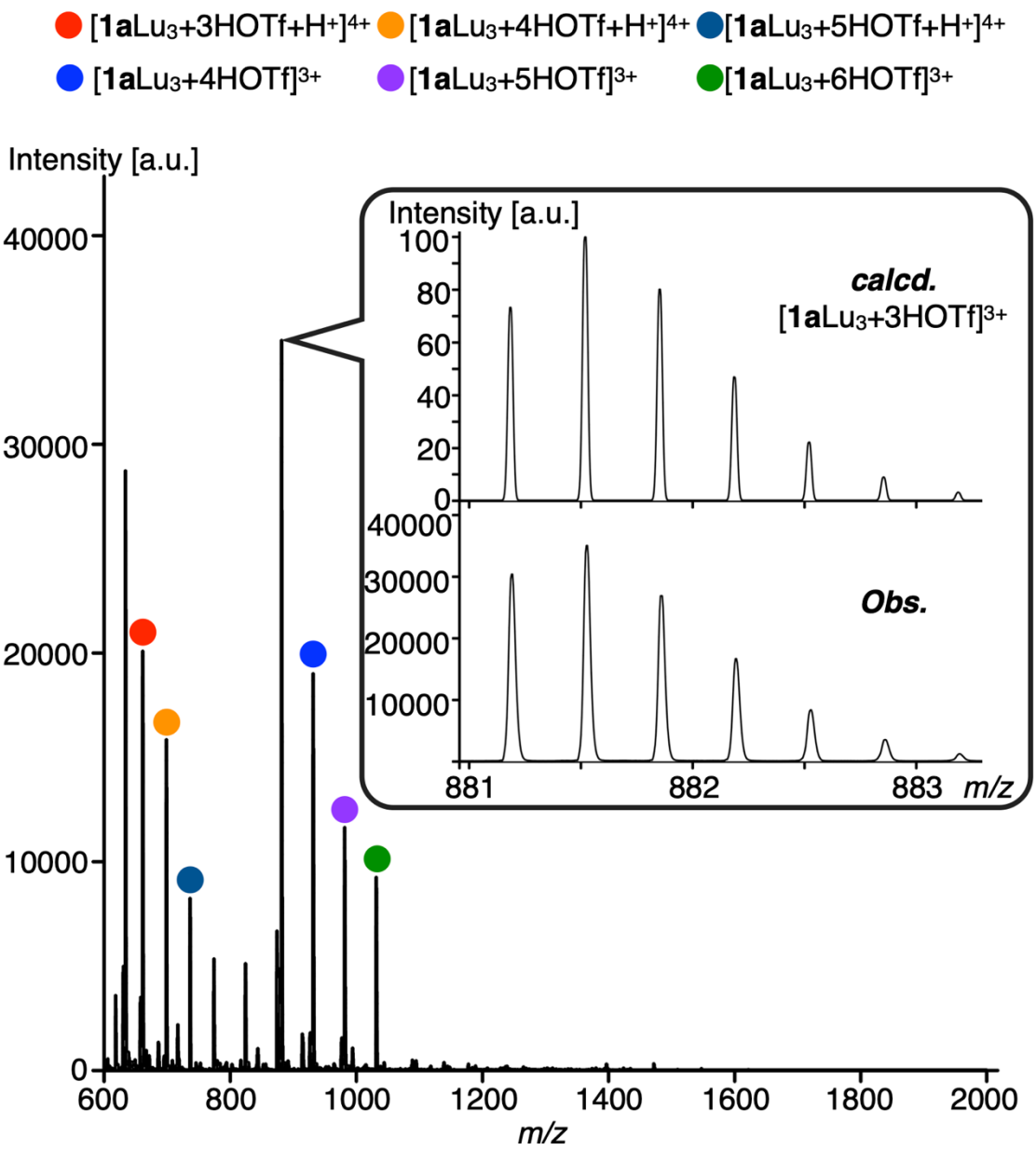

Figure S11. ESI TOF mass spectrum of **1a**Lu_3X_n (positive, CH_3CN, 5 μM).

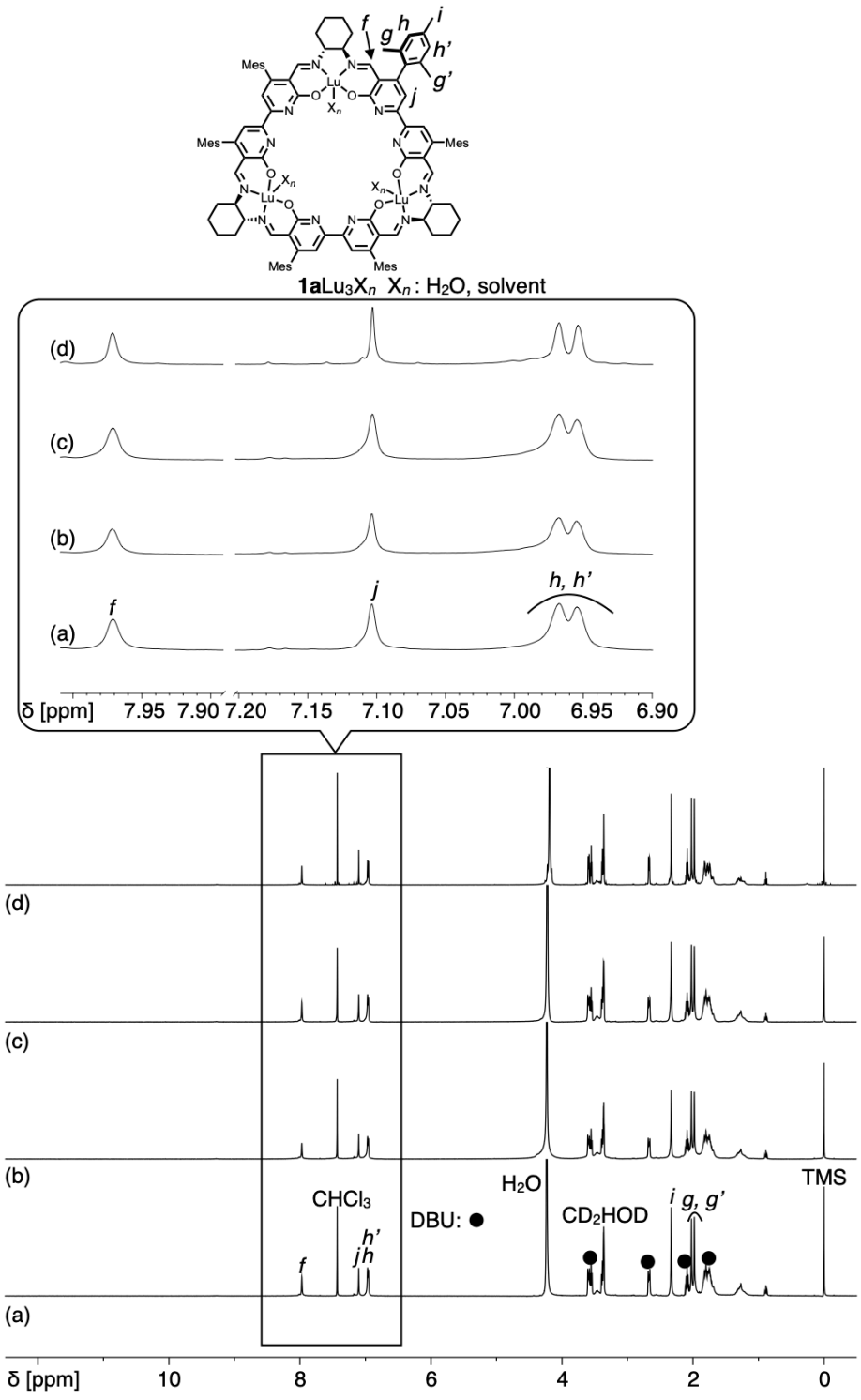

Figure S12. Stability of trinuclear Lu complex at room temperature (^{1}H NMR, $CDCl_3/CD_3OD$ = 3/1, 400 MHz). (a) Trimer **1a**Lu_3X_n prepared from H_6**1a**, $Lu(OTf)_3$, and DBU. (b–d) The sample of (a) stood at r.t. (b) 14 h. (c) 46 h. (d) 72 h.

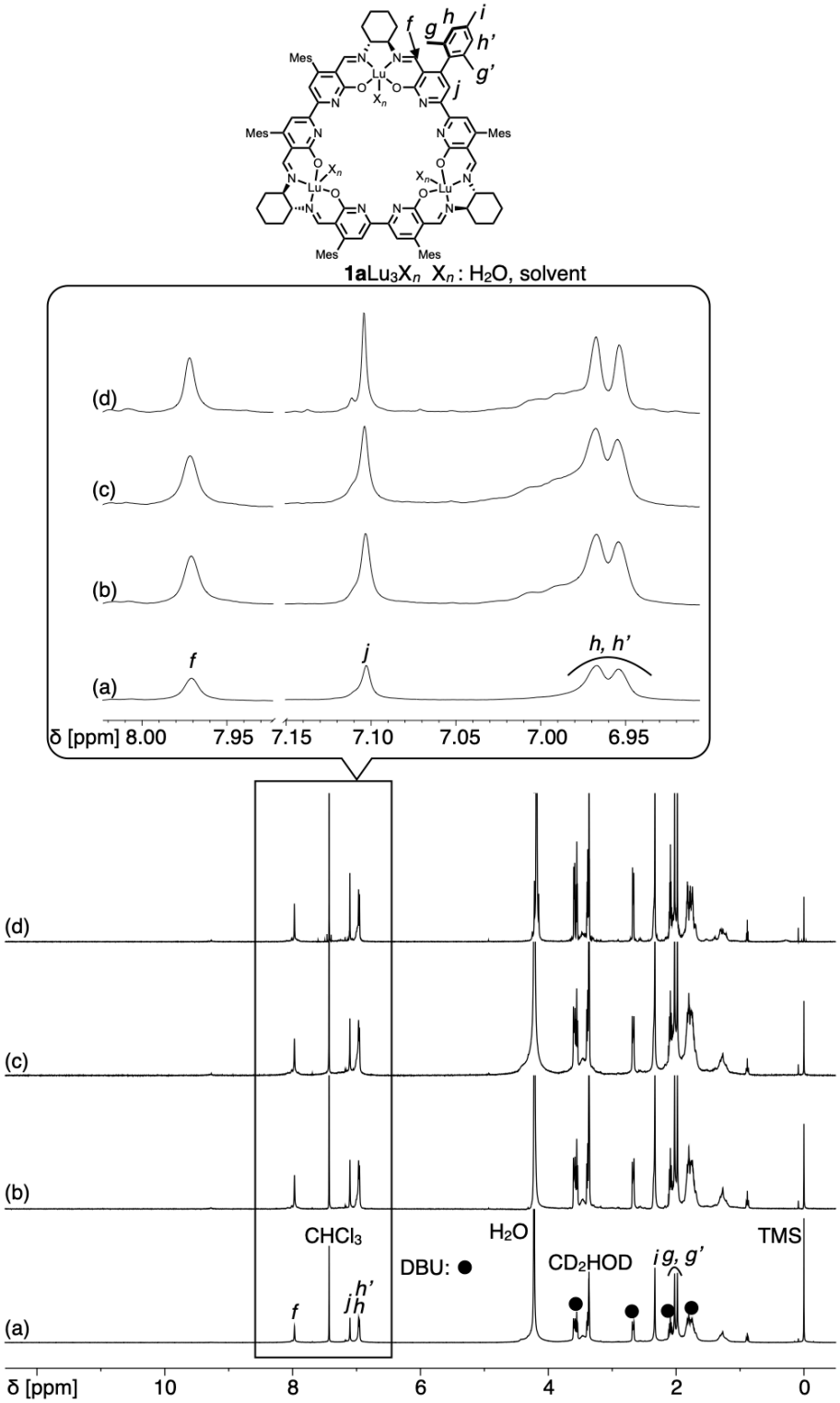

Figure S13. Stability of trinuclear Lu complex at 50 °C (^{1}H NMR, $CDCl_3/CD_3OD$ = 3/1, 400 MHz) (a) Trimer **1a**Lu_3X_n prepared from H_6**1a**, $Lu(OTf)_3$, and DBU. (b–d) The sample of (a) heated at 50 °C. (b) 14 h. (c) 46 h. (d) 72 h.

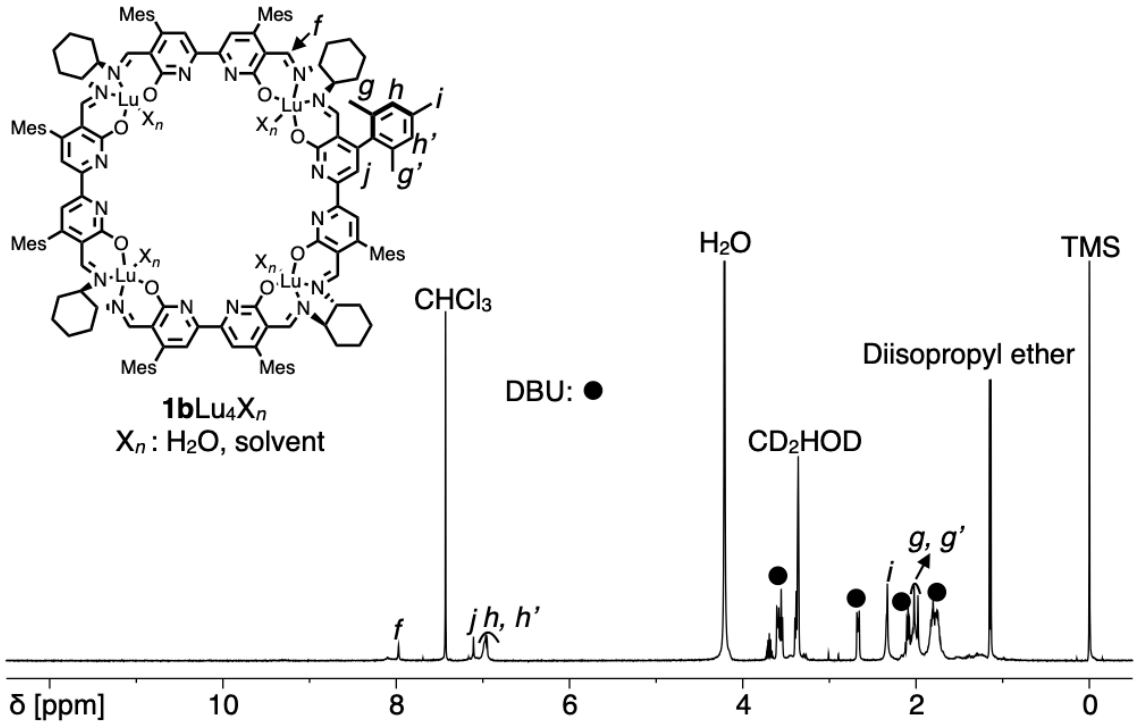

Figure S14. ^{1}H NMR spectrum of **1b**Lu_4X_n (X: H_2O or solvent) ($CDCl_3/CD_3OD$ = 3/1, 600 MHz).

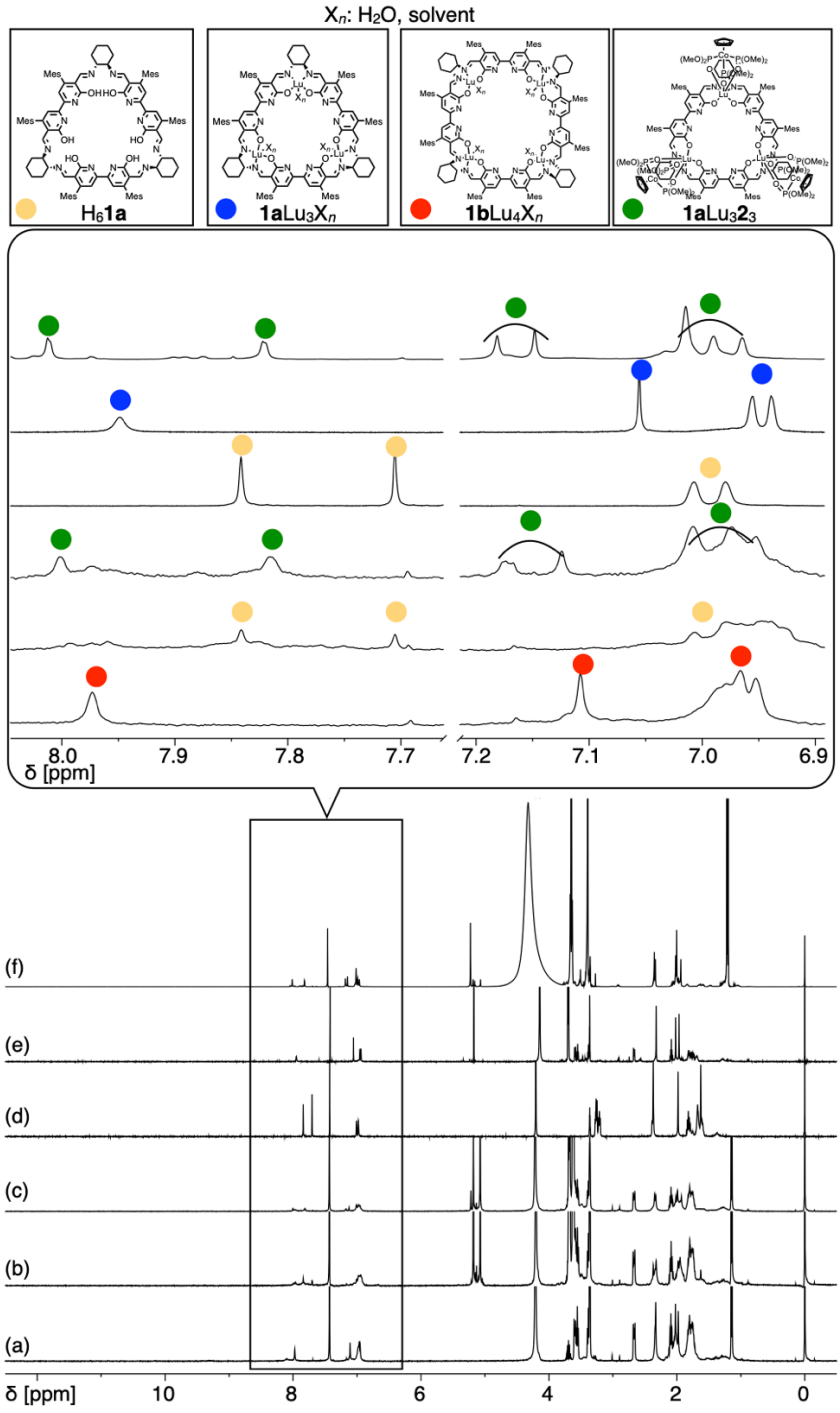

Figure S15. Monitoring the conversion of tetramer **1b**Lu_4X_n to trimer [**1a**Lu_3**2**$_3$] by Kläui ligand (Na**2**) (^{1}H NMR, $CDCl_3/CD_3OD$ = 3/1, 600 MHz). (a) Tetramer **1b**Lu_4X_n prepared by the dissolution of the crystal. (b) After the addition of the Kläui ligand to the sample (a). (c) The sample of (b) stood at r.t. for 12 h. (d) Ligand H_6**1a**. (e) Trimer **1a**Lu_3X_n prepared from H_6**1a** and $Lu(OTf)_3$. (f) [**1a**Lu_3**2**$_3$].

Single crystals of [**1b**$Lu_4(H_2O)_{16}$]$(OTf)_4$ suitable for X-ray diffraction analysis were obtained by slow diffusion of diisopropyl ether vapors into a mixture of H_6**1a**, DBU, and $Lu(OTf)_3$ in $CHCl_3/CH_3OH$ = 3/1.

Crystal data for [**1b**$Lu_4(H_2O)_{16}$]$(OTf)_4$: $C_{148}H_{176}F_{12}Lu_4N_{16}O_{36}S_4$, *Fw* = 3811.16, yellow triangle plate, 0.35 × 0.15 × 0.03 mm^3, orthorhombic, space group *I*222 (No. 23), *a* = 10.4748(6) Å, *b* = 31.6860(15) Å, *c* = 32.6723(16) Å, *V* = 10844.1(10) $Å^3$, θ_{max} = 26.374°, *Z* = 2, R_1 = 0.0679 ($I > 2\sigma$, after SQUEEZE), wR_2 = 0.2024 (all, after SQUEEZE), Flack parameter 0.060(8), GOF = 1.033. CCDC 2374259.

Solvent accessible voids of 2914 cubic angstroms (26.9% of the unit cell volume) were found, where solvent molecules were heavily disordered. The residual electron density was treated with SQUEEZE[S7]. DFIX, DANG, and RIGU, restraints were applied for the atoms of TfO^- anions. DANG and RIGU restraints were applied for a disordered mesityl group. The benzene ring of the disordered mesityl group was fixed with AFIX 66.

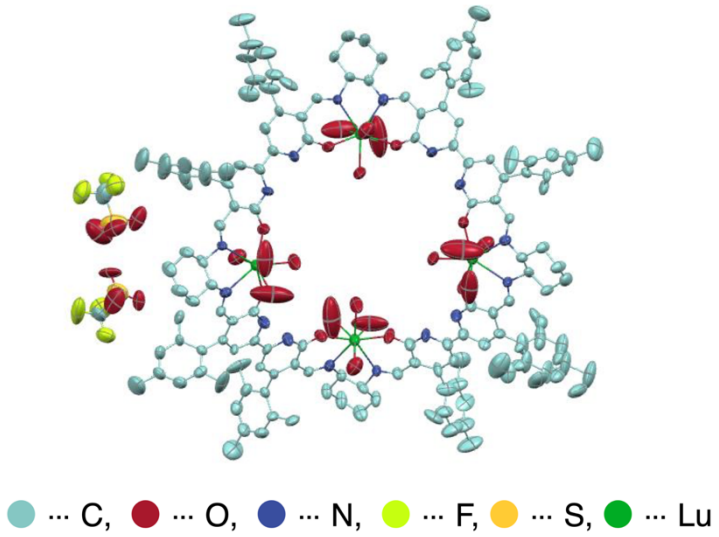

Figure S16. The molecular structure of [**1b**$Lu_4(H_2O)_{16}$]$(OTf)_4$ determined by X-ray diffraction analysis. An ellipsoidal model (50% probability). Hydrogen atoms were omitted for clarity.

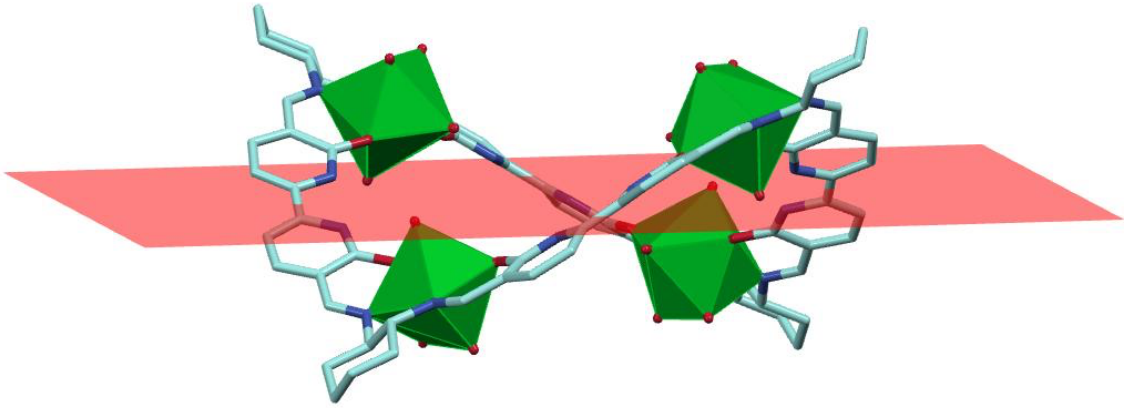

Figure S17. Least-squares plane (red) defined by four Lu atoms of [**1b**$Lu_4(H_2O)_{16}$]$(OTf)_4$.

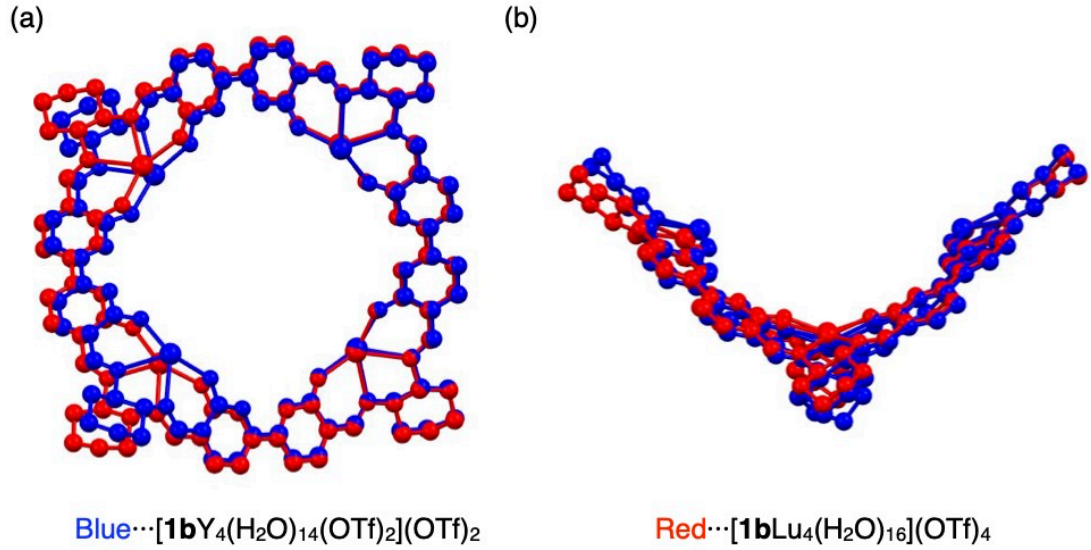

Figure S18. Overlay of structures of [**1b**$Y_4(H_2O)_{14}(OTf)_2$]$(OTf)_2$ and [**1b**$Lu_4(H_2O)_{16}$]$(OTf)_4$ determined by single-crystal X-ray diffraction analysis. (a,b) **1b**Y_4 (blue) and **1b**Lu_4 (red). Solvents, hydrogens, and mesityl groups have been omitted for clarity. (a) Top view. (b) Side view.

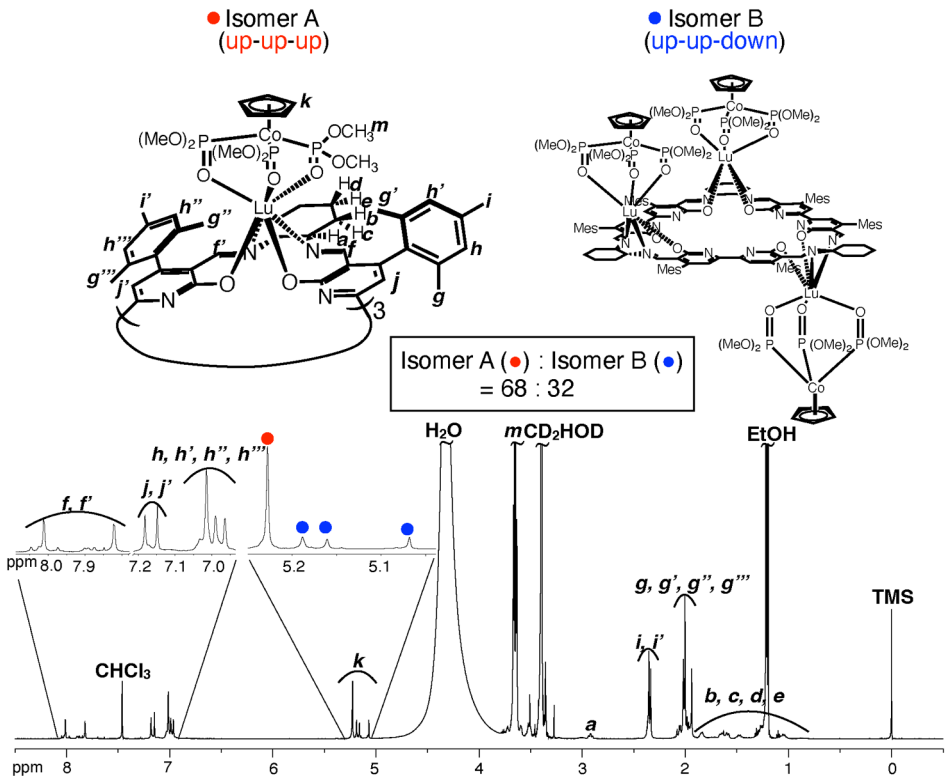

Figure S19. ^{1}H NMR spectrum of [**1a**Lu$_3$**2**$_3$] ($CDCl_3$/CD_3OD = 3/1, 600 MHz).

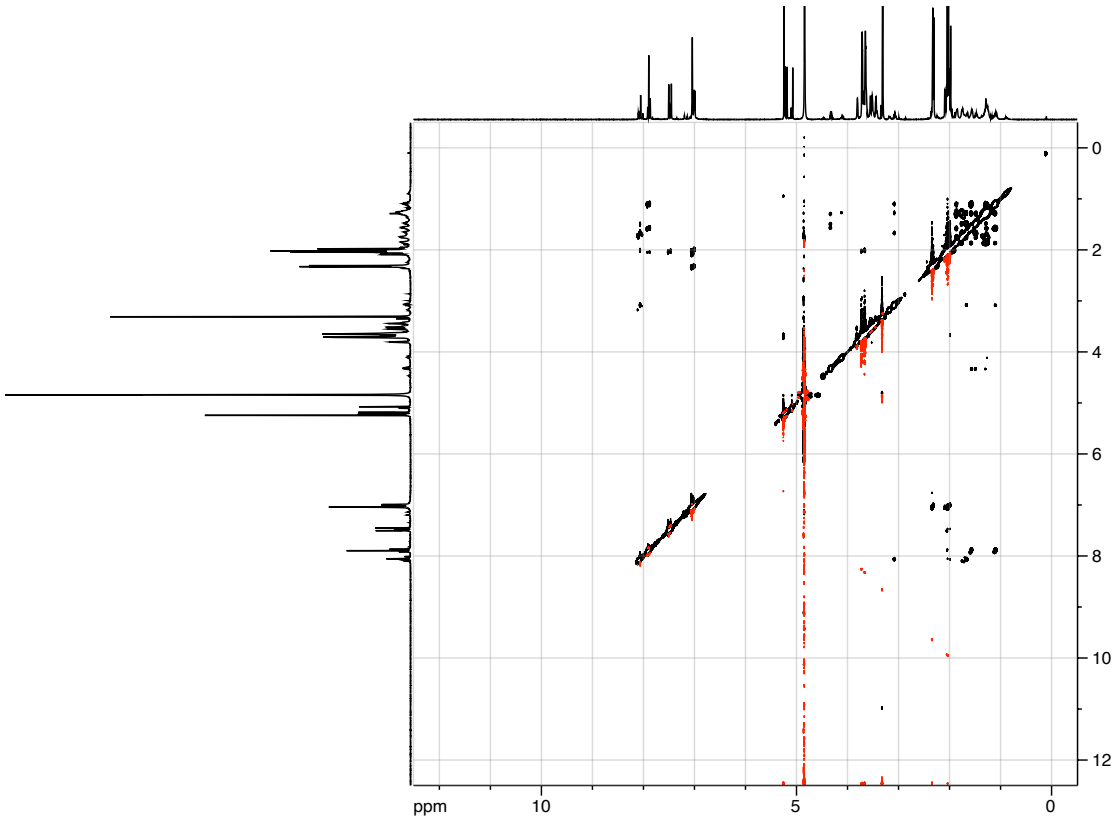

Figure S20. ^{1}H-^{1}H NOESY spectrum of [**1a**Lu_3**2**$_3$] (600 MHz, $CDCl_3/CD_3OD$ = 3/1).

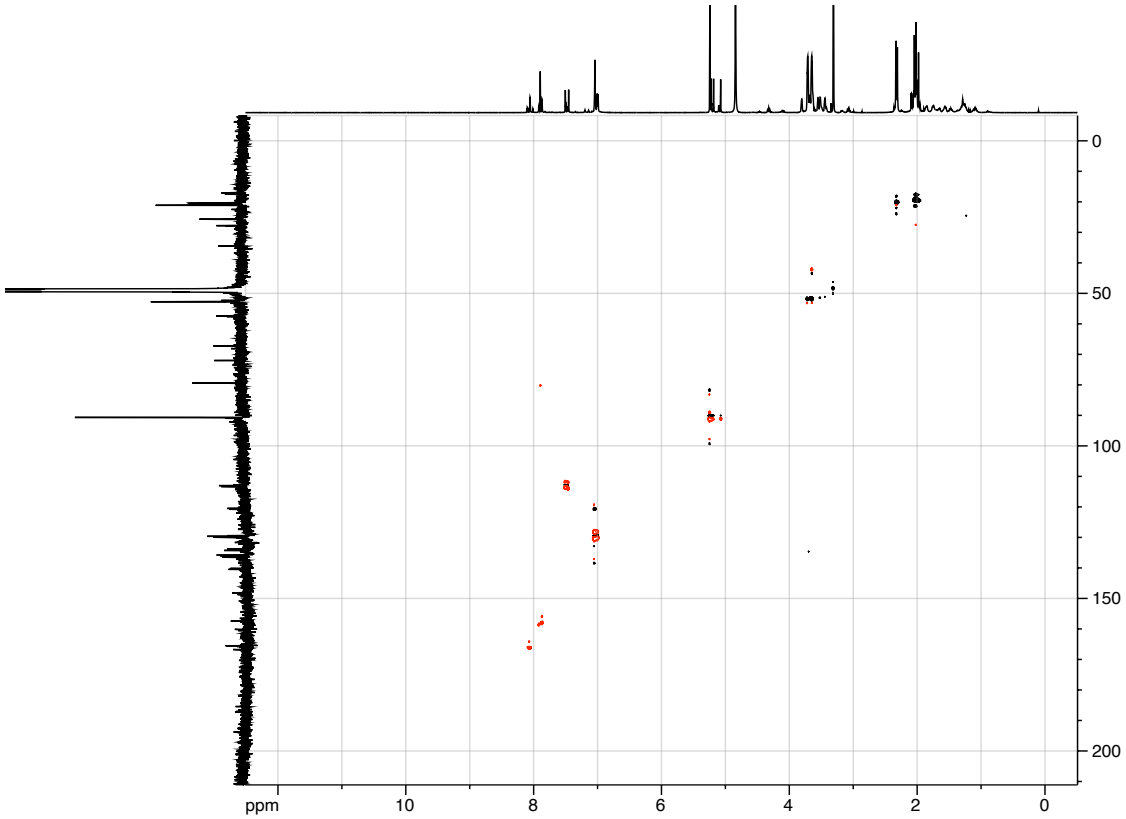

Figure S21. ^{1}H-^{13}C HSQC spectrum of [**1a**Lu_3**2**$_3$] (600 MHz, $CDCl_3/CD_3OD$ = 3/1).

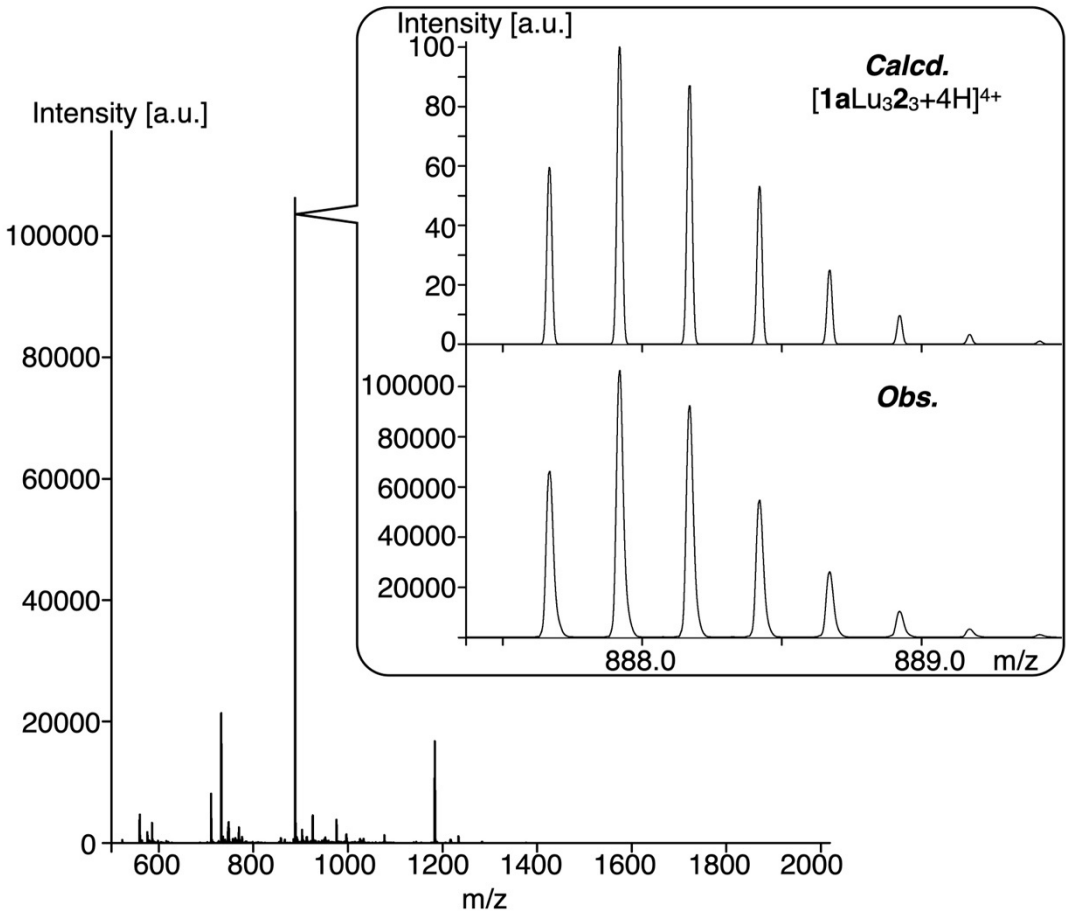

Figure S22. ESI TOF mass spectrum of [**1a**Lu_3**2**$_3$] (positive, CH_3CN, 5 μM).

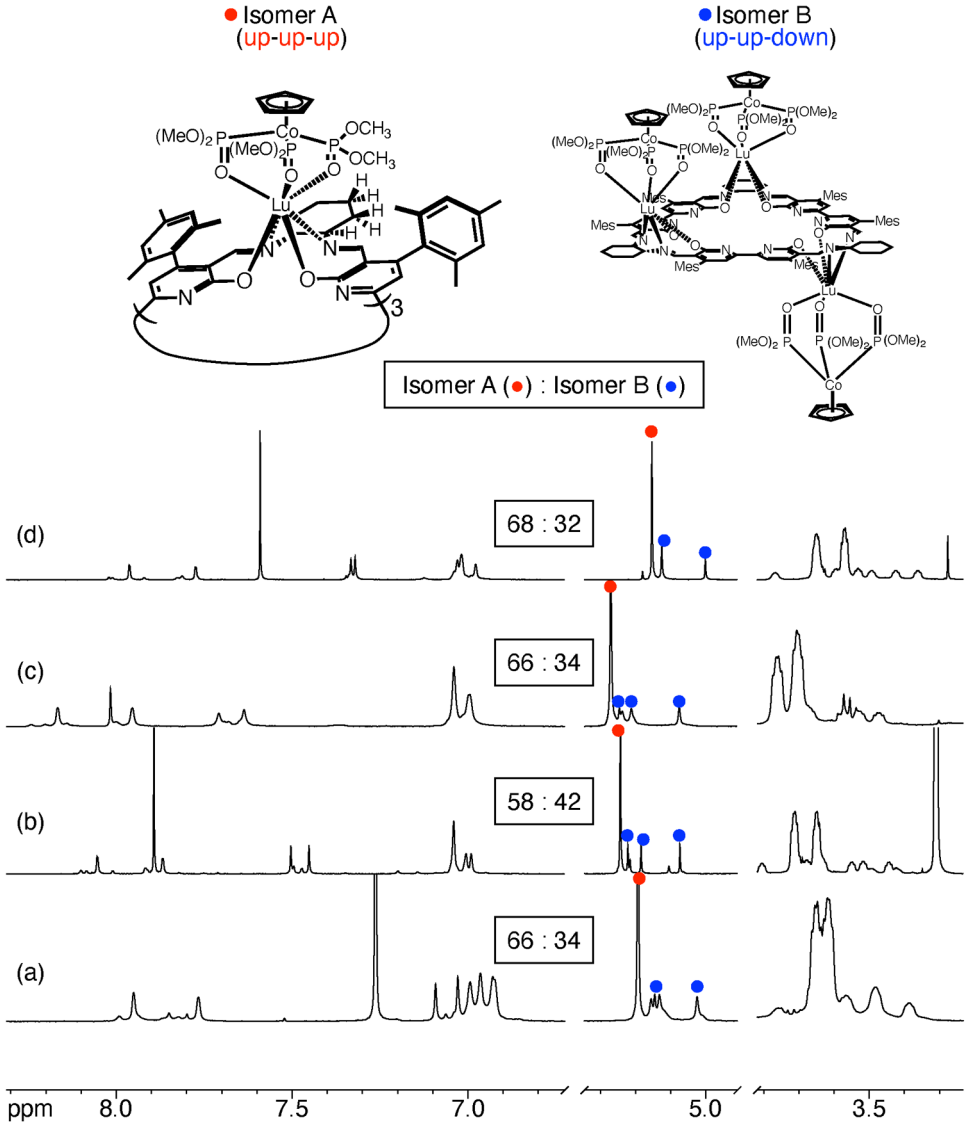

Figure S23. ^{1}H NMR spectra of [**1a**Lu_3**2**$_3$] in different solvents (600 MHz). (a) $CDCl_3$. (b) CD_3OD. (c) Acetone-d_6. (d) CD_3CN.

Single crystals of [**1a**Lu_3**2**$_3$]·3(H_2O) suitable for X-ray diffraction analysis were obtained by slow diffusion of cyclohexane vapors into a $CHCl_3$/CH_3OH = 3/1 solution of [**1a**Lu_3**2**$_3$].

Crystal data for [**1a**Lu_3**2**$_3$]·3(H_2O): $C_{141}H_{183}Co_3Lu_3N_{12}O_{36}P_9$, *Fw* = 3602.41, yellow block , 0.56 × 0.40 × 0.29 mm^3, cubic, space group *I*23 (No 197), *a* = 35.451(3) Å, *V* = 44552(9) Å^3, θ_{max} = 26.361°, *Z* = 8, R_1 = 0.0519 (*I* > 2σ, after SQUEEZE), wR_2 = 0.1429 (all, after SQUEEZE), Flack parameter 0.044(5), GOF = 1.075. CCDC 2374260.

Solvent accessible voids of 18116 cubic angstroms (40.7% of the unit cell volume) were left unfilled, where solvent molecules (chloroform, methanol, cyclohexane, or water) are considered to be severely disordered. The residual electron density was treated with SQUEEZE[S7]. DFIX, DANG, and RIGU restraints were applied for the $P(OMe)_2$ groups.

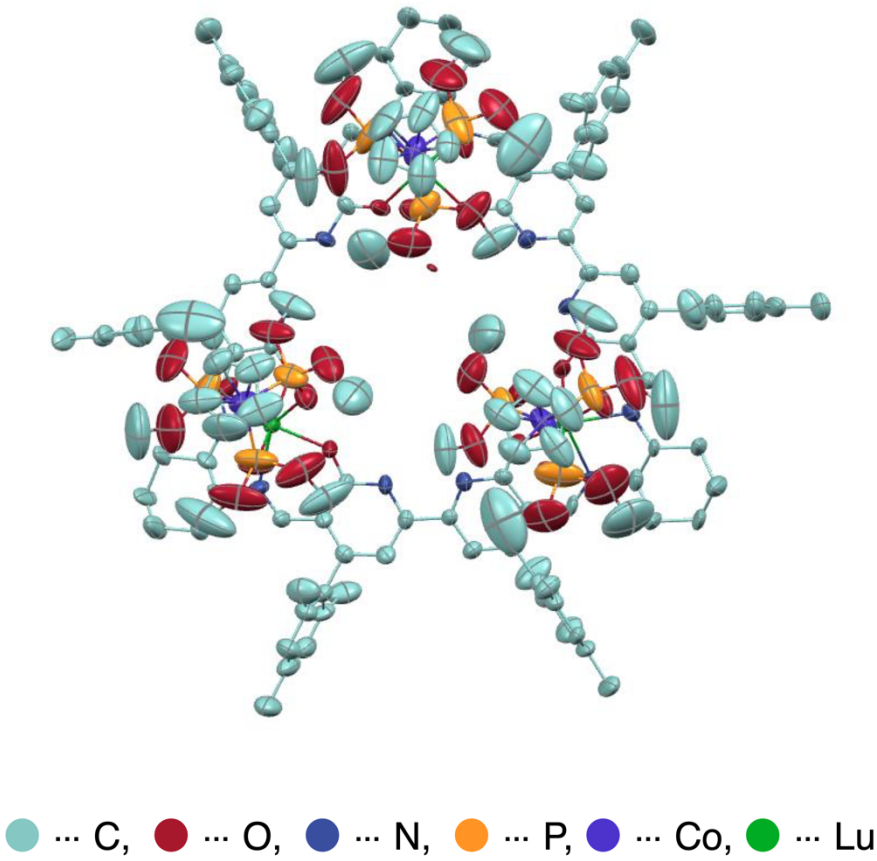

Figure S24. The molecular structure of [**1a**Lu_3**2**$_3$]·(H_2O) determined by X-ray diffraction analysis. An ellipsoidal model (50% probability). Hydrogen atoms were omitted for clarity.

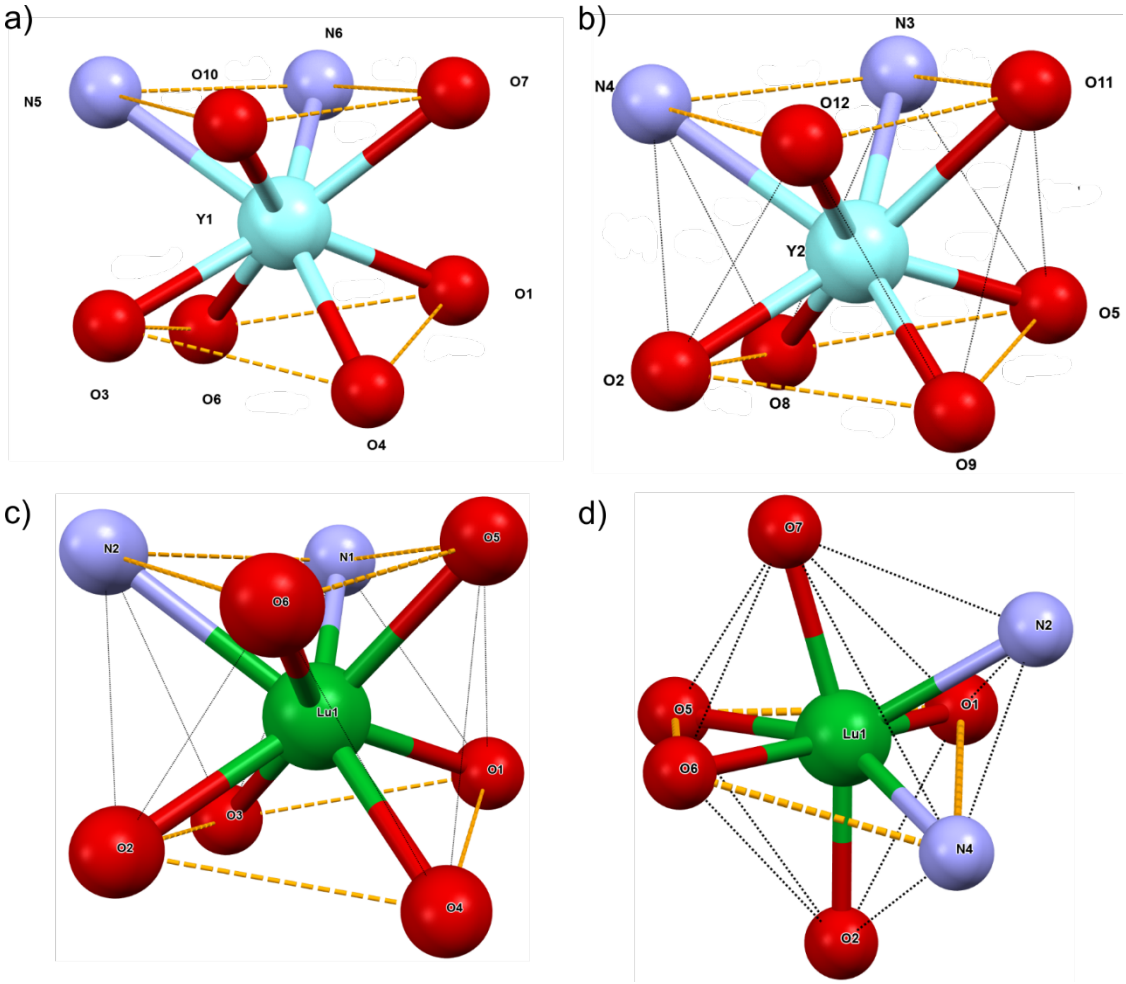

Figure S25. Coordination polyhedra of the rare earth cores in their complexes with macrocycles **1a** and **1b** showing distorted square antiprismatic geometries for [**1b**$Y_4(H_2O)_{14}(OTf)_2](OTf)_2$ (a,b) and [**1b**$Lu_4(H_2O)_{16}](OTf)_4$ (c) and distorted mono-capped octahedral geometries for [**1a**Lu_3**2**$_3$] (d).

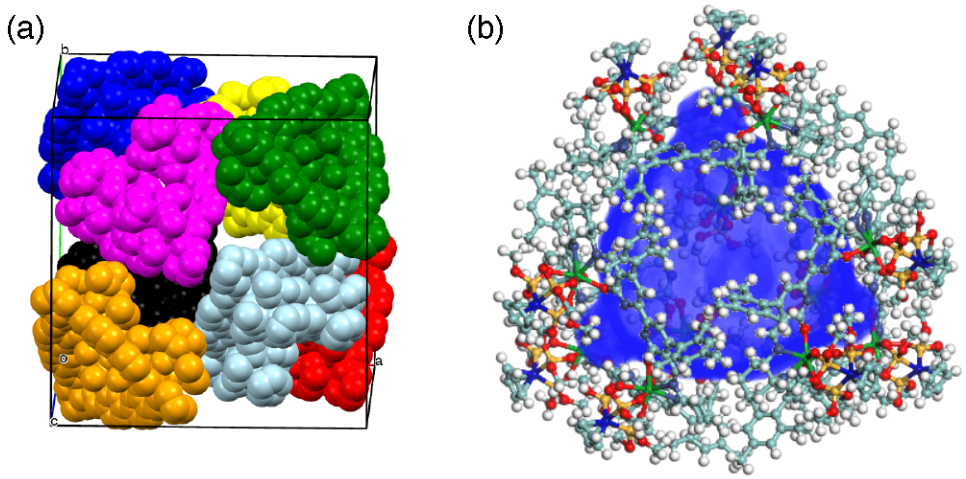

Figure S26. Structure of [**1a**Lu_3**2**$_3$] determined by single-crystal X-ray diffraction analysis. Solvents, hydrogens, and mesityl groups have been omitted for clarity in (a–b). (a,b) Packing of eight [**1a**Lu_3**2**$_3$]. (a) Space-fill model. (b) Intermolecular voids.

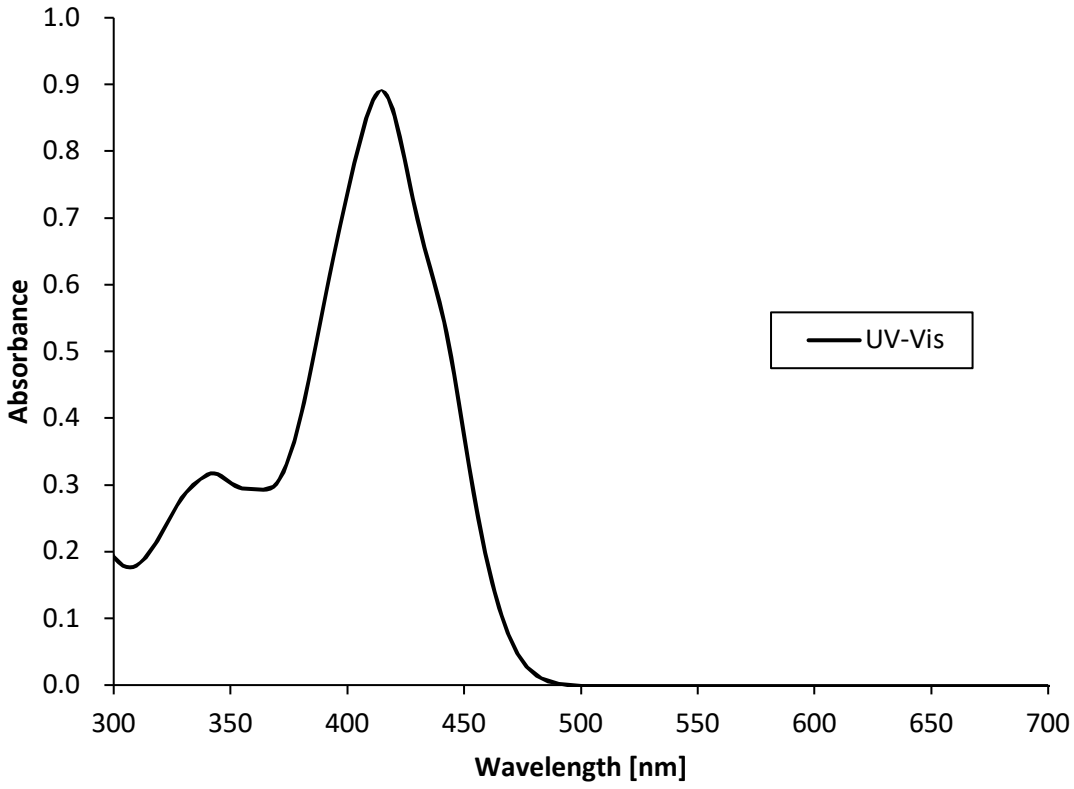

Figure S27. Absorption spectrum of [**1a**Lu_3**2**$_3$] ($CHCl_3$, 10 μM, l = 1 cm).

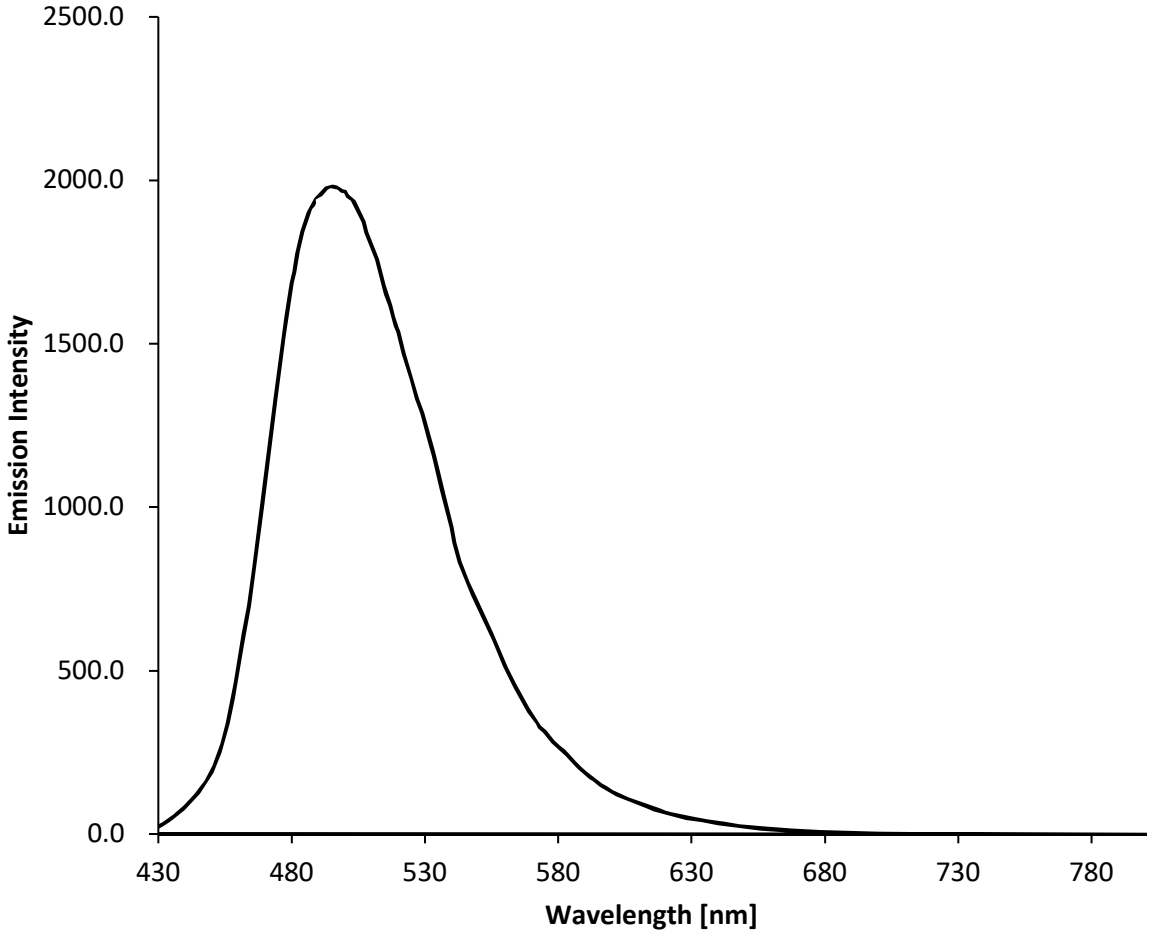

Figure S28. Emission spectrum of [**1a**Lu_3**2**$_3$] ($CHCl_3$, 10 μM, l = 1 cm, λ_{ex} = 414 nm, excitation slit = 5 nm, emission slit = 5 nm). Absolute emission quantum yields in the same condition was 5.4%.

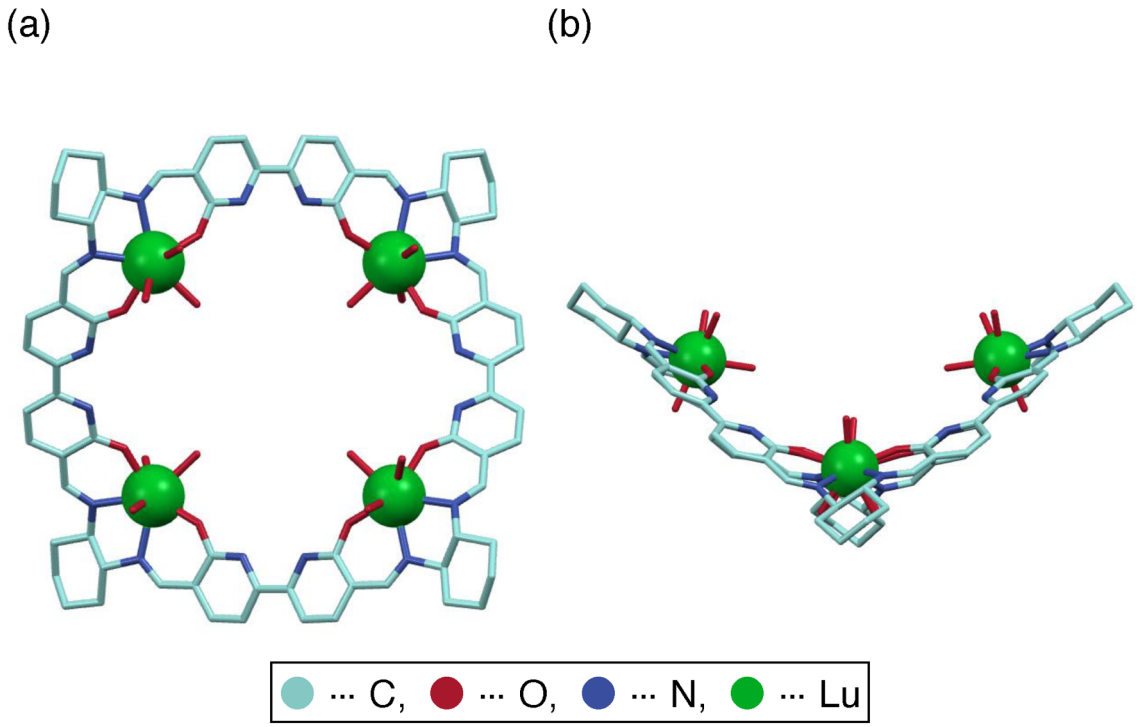

Figure S29. Lutetium tetramer complex. (a,b) Structure of [**1b**$Lu_4(H_2O)_{16}$]$(OTf)_4$ determined by single-crystal X-ray diffraction analysis. Solvents, TfO^- anions, hydrogens, and mesityl groups have been omitted for clarity. Ball-and-stick models. (a) Top (b) Side.

References for the Supplementary Information

S1. (a) Bruker, APEX2, 2014. (b) Bruker, APEX3, 2019.

S2. (a) K. Wakita, Yadokari-XG, Software for Crystal Structure Analyses, 2001. (b) C. Kabuto, S. Akine, T. Nemoto, E. Kwon, *J. Cryst. Soc. Jpn.*, 2009, **51**, 218–224.

S3. G. M. Sheldrick, *Acta Cryst.*, 2008, **A64**, 112–122.

S4. G. M. Sheldrick, *Acta Cryst.* 2015, **C71**, 3–8.

S5. T. Nakamura, Y. Kawashima, E. Nishibori and T. Nabeshima, *Inorg. Chem.*, 2019, **58**, 7863–7872.

S6. W. Kläui, W. Eberspach and P. Gütlich, *Inorg. Chem.* 1987, **26**, 3977–3982.

S7. A. L. Spek, *Acta Cryst.* 2009, **D65**, 148–155.